Environmental Science Processes & Impacts

PAPER

View Article Online
View Journal

Cite this: DOI: 10.1039/d2em00184e

Impact of beaver ponds on biogeochemistry of organic carbon and nitrogen along a fire-impacted stream†

Holly K. Roth, [a] Amelia R. Nelson, [b] Amy M. McKenna,[bc] Timothy S. Fegel,[d] Robert B. Young, [e] Charles C. Rhoades,[d] Michael J. Wilkins[b] and Thomas Borch *[ab]

Wildfires, which are increasing in frequency and severity in the western U.S., impact water quality through increases in erosion, and transport of nutrients and metals. Meanwhile, beaver populations have been increasing since the early 1900s, and the ponds they create slow or impound hydrologic and elemental fluxes, increase soil saturation, and have a high potential to transform redox active elements (*e.g.*, oxygen, nitrogen, sulfur, and metals). However, it remains unknown how the presence of beaver ponds in burned watersheds may impact retention and transformation of chemical constituents originating in burned uplands (*e.g.*, pyrogenic dissolved organic matter; pyDOM) and the consequences for downstream water quality. Here, we investigate the impact of beaver ponds on the chemical properties and molecular composition of dissolved forms of C and N, and the microbial functional potential encoded within these environments. The chemistry and microbiology of surface water and sediment changed along a stream sequence starting upstream of fire and flowing through multiple beaver ponds and interconnecting stream reaches within a burned high-elevation forest watershed. The relative abundance of N-containing compounds increased in surface water of the burned beaver ponds, which corresponded to lower C/N and O/C, and higher aromaticity as characterized by Fourier transform ion cyclotron resonance mass spectrometry (FT-ICR MS). The resident microbial communities lack the capacity to process such aromatic pyDOM, though genomic analyses demonstrate their potential to metabolize various compounds in the anaerobic sediments of the beaver ponds. Collectively, this work highlights the role of beaver ponds as biological "hotspots" with unique biogeochemistry in fire-impacted systems.

Received 30th April 2022
Accepted 11th August 2022

DOI: 10.1039/d2em00184e

rsc.li/espi

Environmental significance

Beaver populations in North America have been increasing since the early 1900s, as have the occurrence of wildfires in the western U.S., causing beaver ponds to be frequently present within fire impacted watersheds. Thus, it is important to understand how beaver ponds control the retention and transformation of fire-affected organic matter. Here, we analyzed a series of beaver ponds and interconnecting free-flowing streams affected by the 2018 Ryan Fire in Wyoming, USA. We found that fire-impacted organic matter, rich in nitrogen, accumulated within the beaver ponds. We also investigated the microbial communities present in fire-impacted beaver ponds, which has not been previously reported. Our data indicates that beaver ponds function as biogeochemical hotspots controlling downstream water quality within burned watersheds.

1. Introduction

Forests provide ecosystem services valued at ~$5 trillion annually[1–3] and are critical global sources of high-quality drinking water.[4,5] Wetlands contribute to these services, as they filter water, influence biogeochemical cycling, and support local flora and fauna.[5] Such services are susceptible to natural or anthropogenic disturbances (*e.g.*, wildfire, insect infestation, development, *etc.*), especially as such disruptions may threaten downstream water quality.[6] Wildfires are of particular concern in the western U.S., as their frequency, intensity, and duration

[a]*Department of Chemistry, Colorado State University, Fort Collins, CO, USA. E-mail: Thomas.borch@colostate.edu; Tel: +1-970-491-6235*

[b]*Department of Soil and Crop Sciences, Colorado State University, Fort Collins, CO, USA*

[c]*National High Magnetic Field Laboratory, Ion Cyclotron Resonance Facility, Florida State University, FL, USA*

[d]*Rocky Mountain Research Station, U.S. Forest Service, Fort Collins, CO, USA*

[e]*Chemical Analysis & Instrumentation Laboratory, New Mexico State University, Las Cruces, NM, USA*

† Electronic supplementary information (ESI) available. See https://doi.org/10.1039/d2em00184e

have increased in recent years and are projected to increase further.[7,8] This underscores the need to better understand the consequences of severe fire on the ecosystem processes that regulate clean water supply.

Heating and combustion of organic matter during severe wildfires creates pyrogenic organic matter (pyOM),[9] comprised of char, soot, and condensed polycyclic aromatic molecules, and accounts for ~5–15% of soil carbon.[10] The higher hydrophobicity and aromaticity, lower C : N ratios, and longer mean residence times of C in pyOM alters biogeochemical processes compared to unburned soils.[11–13] pyOM may be introduced to fluvial systems in post-fire runoff, which can be enriched in dissolved organic carbon (DOC), nitrogen (N), heavy metals, nutrients, and polycyclic aromatic hydrocarbons.[14–16] Indeed, stream DOC concentrations often increase following fire,[17–19] though its reactivity and impacts on either river microbial communities or water treatment is less certain. Recent studies document elevated post-fire DOC with increased aromaticity and aromatic carboxylic acid concentrations,[20,21] though a comprehensive molecular-level characterization of these compounds is lacking. Shifts to more recalcitrant functional groups may inhibit microbial metabolism of DOC[22,23] and preserve pyOM within aquatic ecosystems. Further, exported pyOM from burned catchments is known to have costly short- and long-term impacts on downstream drinking water treatment and aquatic ecosystems.[6,24] Wildfire effects on water quality can persist for years,[15] and therefore represent important financial and functional challenges for water treatment.[10]

Concurrent to increases in fire activity, North American beaver (*Castor canadensis*) populations have steadily increased since their near eradication in the northern U.S. in the early 1900s.[25] These "ecosystem engineers" build dams and create channels which influence hydrologic and biogeochemical processes with relevance to downstream water quality.[26,27] The structure of beaver dams and associated physical features are known to influence post-fire stream channel and floodplain geomorphology,[32] but their impact on microbial communities and biogeochemical processes remains poorly studied.[30] Beaver dams and the floodplain complexity they create trap particulate carbon (C) and nutrients and create reduced zones that are depleted in dissolved oxygen,[27] where microbes must rely on alternate electron acceptors for respiration (*e.g.*, NO_3^-, Fe^{3+}).[28] Tied to these biogeochemical changes, beaver ponds influence the availability of nutrients, solubility of metals, and quality of C in surface waters and sediments,[25,29,30] likely affecting C and N dynamics.[31,32] In contrast to free-flowing stream reaches that favor aerobic respiration, the reducing conditions within beaver ponds favor anaerobic metabolisms. Microbes are known to metabolize pyOM in well-oxygenated soils,[33,34] but the potential for microbial processing of pyOM under saturated beaver pond anoxic conditions is less well understood. With beaver populations reaching approximately 30 million in North America[35] and over 1 million in Eurasia,[36] understanding the influence of beaver ponds on pyOM processing is critical to predict C and N cycling in impacted areas.

Nitrogen is a limiting reactant for microbial and plant productivity,[37,38] and its lability and bioavailability are sensitive to both heating and postfire ecosystem characteristics.[39,40] Although dissolved nitrogen can remain elevated in streams for years following fire,[41–43] little is known about the biotic (*e.g.*, nitrification, dissimilatory nitrate reduction to ammonium) or abiotic (*e.g.*, sorption, aggregation) processes that regulate soil N cycling and release to surface water.[44] Fourier transform ion cyclotron resonance mass spectrometry (FT-ICR MS) coupled with electrospray ionization analysis shows that combustion during wildfire creates thermodynamically recalcitrant organic matter that resists microbial degradation and alters C and N cycling.[45–47] FT-ICR MS permits direct measurement of DON and has shown that the N contained in pyOM is incorporated into refractory, heterocyclic aromatic compounds.[44,46,48,49] However, molecular

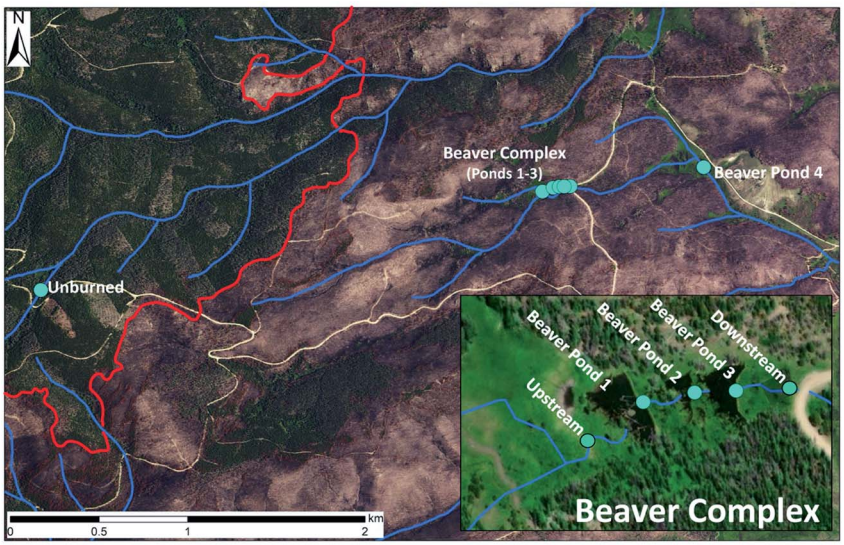

Fig. 1 Sampling locations along Middle Fork of Big Creek within the Ryan Fire near the Colorado–Wyoming border and unburned subalpine forest along a tributary of McAnulty Creek.

transformations which may occur to nitrogenated pyOM in anoxic conditions are not not-well known, despite the implications they may have for N cycling.[50,51]

This work investigates potential post-fire changes to surface water C and N chemistry and sediment microbiome composition and function within beaver ponds. Work was conducted in a subalpine forest watershed within the Medicine Bow-Routt National Forest, Wyoming, USA, that burned during the 2018 Ryan Fire. We collected surface water and sediment samples along a series of beaver ponds within a severely burned portion of the watershed (Fig. 1). We expected to find higher N concentrations and DOM with higher aromaticity and larger molecular sizes in the beaver ponds compared to free-flowing stream reaches. We hypothesized that changes in surface water molecular speciation would influence microbial communities in beaver pond sediments. Finally, we examined whether microbially mediated biogeochemical processes influence C and N composition or export from fire-affected beaver ponds.

2. Methods

2.1 Site description, sample collection and processing

Surface water was collected at six locations along a burned stream affected by the 2018 Ryan Fire (Middle Fork of Big Creek) starting above a series of four beaver ponds and from an adjacent unburned tributary of McAnulty Creek (Fig. 1). Three neighboring ponds were combined and analyzed as a complex, whereas Pond 4 was 3.5 km downstream and was analyzed separately. Surface grab samples (one per sampling location) were collected monthly starting near peak runoff throughout the summer (mid-June through October) one and two years postfire. Stream water samples were collected from the thalweg of the stream and pond samples were collected near the outlet at the sediment–water interface.

Because water chemistry and the environmental microbiome are intimately connected, we used DNA-based methods to characterize the beaver pond microbiome within our sampling sites and adjacent wetlands outside of the Ryan Fire (Fig. S1†). Based on year 1 observations, we sampled bulk surficial sediments and associated pore water from Beaver Ponds 1, 2, and 4, along with 4 other beaver ponds in adjacent watersheds in the fall of 2020, for a total of seven samples. We additionally attempted to collect only porewater samples from the ponds, but the sediment in the ponds was very fine and all attempts to use porewater "sippers" resulted in them clogging without yielding sufficient sample for analysis. Therefore, surficial sediment and pore water samples (approximately 5 cm depth) were collected from the sediment–water interface using an ethanol-sterilized plastic cup and stored in a cooler for transport. One sediment sample was collected per sampling location.

2.2 Carbon, nitrogen, and UV-Vis fluorescence

Water samples analyzed for DOC, DTN, and UV-Vis fluorescence spectroscopy were collected in pre-combusted (heated for 3 hours at 500 °C) glass amber bottles and filtered through 0.7 μm pore-size glass fiber filters (Millipore Corp, Burlington, MA) within 24 hours of collection. Samples for anion and cation analyses were collected in opaque high-density polyethylene (HDPE) plastic bottles after triple washing with de-ionized water (EC < 1.0 μS cm^{-1}).

DOC and DTN measurements were performed *via* high-temperature combustion catalytic oxidation on a Shimadzu TOC-VCPN total organic C/N analyzer with 2 M HCl addition before analysis to remove mineral C (Shimadzu Corporation, Columbia, MD). Inorganic nutrient concentrations were determined by ion chromatography *via* electrical conductivity detection, using an AS19A Anion-Exchange column for anions and a CS12A Cation-Exchange column for cations (Dionex Corp, Sunnyvale, CA, APHA, 1998a). Detection limits for NO_3^- and NH_4^+ were 10 μg L^{-1}. DON is estimated as the difference between DTN and the sum of dissolved inorganic N forms ($NO_3^-N + NH_4^+–N$).

Optical parameters, such as fluorescence index (FI), and freshness index (β/α) approximate DOM characteristics, (*e.g.*, aromaticity, degree of microbial processing) to measure shifts in DOM composition.[50] Although these parameters only reflect the fluorophores in the sample, they can be used to determine variations in DOM source and biogeochemical processes.[51,52] FI is widely applied in stream water and wildfire studies, as it appears to be particularly sensitive for wildfire-impacted DOM due to increases in oxidized functional groups (increased by ~0.13 in fire-impacted sediment leachates).[53] Samples were analyzed using a Horiba Scientific Aqualog (Horiba-Jobin Yvon Scientific Edison, New Jersey, US) with excitation and emission wavelengths from 200–800 nm at 3 nm intervals and scan times of 2 seconds. Filtered samples were diluted to 5 mg C L^{-1} prior to analysis to reduce inner-filter effects and normalize their concentrations. A sealed cuvette of deionized water was used as a blank and analyzed between every ten samples to correct for instrument drift. The samples were corrected for inner-filter effects and Rayleigh scatter was masked using first and second grating orders after spectral analysis. Finally, each spectrum was normalized by the area of the deionized water Raman scattering peak, as determined by the blank.[54] From this, fluorescence index (FI, eqn (1)),[50] and freshness index were calculated (β/α, eqn (2)).[55]

$$\mathrm{FI} = \text{excitation: } 370 \text{ nm, emission } \frac{470 \text{ nm}}{520 \text{ nm}} \quad (1)$$

$$\beta/\alpha = \frac{\text{beta(excitation: 310 nm, emission 380 nm)}}{\text{alpha(excitation: 310 nm, emission max intensity between 420} - \text{435 nm)}} \quad (2)$$

2.3 Fourier transform ion cyclotron resonance mass spectrometry

2.3.1 Sample preparation. Compositional analysis of the water samples was conducted using 21 tesla FT-ICR MS, used to further explore the differences in DOM composition which cannot be determined by concentration alone. The 21T FT-ICR mass spectrometer achieves high resolving power ($m/\Delta m_{50\%}$ = 3 000 000 at m/z 200), sub-ppm mass accuracy (20–80 ppb), and high dynamic ranges that allows the assignment of tens of thousands of species per mass spectrum.[56–58] To extend compositional coverage, we applied both positive-ion (+ESI) and negative-ion electrospray ionization (−ESI) to selectively ionize basic/acidic polar species through protonation/deprotonation.[46,59]

Water samples collected in June 2019 were extracted for FT-ICR MS analysis, with each beaver pond in the beaver complex analyzed separately to evaluate the effect of different retention times on chemical composition. Samples for FT-ICR MS analysis were collected in pre-combusted (heated for 6 hours at 400 °C) glass amber bottles, filtered through 0.2 μm polyether sulfone filters and stored at 4 °C to minimize microbial activity. Prior to FT-ICR MS analysis, samples were prepared *via* solid phase extraction according to Dittmar *et al.*, 2008.[60] Briefly, 500 mL of each sample was acidified to pH 2 using trace metal-grade HCl (Sigma-Aldrich Chemical Co.). Agilent Bond Elut PPL cartridges (3 mL, 200 mg) were prepared by rinsing first with 15 mL methanol followed by 15 mL pH 2 water. PPL cartridges are a common SPE sorbent, as they are selective for polar compounds that are prevalent in OM.[61] PPL selectivity and high extraction efficiency (approximately 40–65% DOC recovery) made them an appropriate sorbent for this analysis.[62] Each water sample was passed through a PPL cartridge that was subsequently rinsed with 15 mL pH 2 water to remove salts. Finally, each sample was eluted with 2 mL HPLC grade methanol (Sigma-Aldrich Chemical Co., St. Louis, MO). SPE extracts were ran without further dilution prior to analysis by negative and positive ion electrospray ionization (ESI).[46]

2.3.2 Instrumentation: ESI source. The sample solution was infused *via* a micro electrospray source[63] (50 μm i.d. fused silica emitter) at 500 nL min^{-1} by a syringe pump. Typical conditions for negative ion formation were: emitter voltage, −2.7–3.2 kV; S-lens RF (45%) and heated metal capillary temperature 350 °C. Positive-ion ESI spray conditions were opposite in polarity.

2.3.3 Instrumentation: 21 T FT-ICR MS. SPE extracts were analyzed with a custom-built hybrid linear ion trap FT-ICR mass spectrometer equipped with a 21 T superconducting solenoid magnet.[58,64] Ions were initially accumulated in an external multipole ion guide (1–5 ms) and released m/z-dependently by decrease of an auxiliary radio frequency potential between the multipole rods and the end-cap electrode.[65] Ions were excited to m/z dependent radius to maximize the dynamic range and number of observed mass spectral peaks (32–64%),[65] and excitation and detection were performed on the same pair of electrodes.[66] The dynamically harmonized ICR cell in the 21 T FT-ICR is operated with 6 V trapping potential.[65,67] Time-domain transients of 3.1 seconds were acquired with the Predator data station that handled excitation and detection only, initiated by a TTL trigger from the commercial Thermo data station, with 100 time-domain acquisitions conditionally-coadded for all experiments.[68] Mass spectra were phase-corrected[69] and internally calibrated with 10–15 highly abundant homologous series that span the entire molecular weight distribution based on the "walking" calibration method.[70] Mass spectral peaks with signal magnitude greater than six-times the baseline root-mean-square noise level at m/z 500 were exported to a peak list. Experimentally measured masses were converted from the International Union of Pure and Applied Chemistry (IUPAC) mass scale to the Kendrick mass scale[71] for rapid identification of homologous series for each heteroatom class (*i.e.*, species with the same $C_cH_hN_nO_oS_s$ content, differing only by degree of alkylation).[72] For each elemental composition, $C_cH_hN_nO_oS_s$, heteroatom class, double bond equivalents (DBE = number of rings plus double bonds to C, $DBE = C - h/2 + n/2 + 1$)[73] and C number, c, were tabulated for subsequent generation of heteroatom class relative abundance distributions and graphical relative-abundance weighted images and van Krevelen diagrams. Molecular formula assignments and data visualization were performed with PetroOrg© software.[74] Molecular formula assignments with an error >0.25 parts per million were discarded, and only chemical classes with a combined relative abundance of ≥0.15% of the total were considered. All FT-ICR MS spectra are publicly available through the Open Science Framework (**https://osf.io/t4eqx/**) (**https://doi.org/10.17605/OSF.IO/T4EQX**).

2.3.4 Molecular formula calculations. Assigned elemental compositions from neutral species were used to calculate O/C and C/N ratios, modified aromaticity index (AI_{mod}; eqn (3)),[75,76] and nominal oxidation state of carbon (NOSC; eqn (4)).[77] Van Krevelen diagrams were also constructed from the FT-ICR MS results, in which the elemental ratio of O/C is plotted on the x-axis and the H/C ratio is plotted on the y-axis to visualize the spread of the assigned formulas and major compositional shifts.[78]

$$AI_{mod} = \frac{1 + C - \frac{1}{2}O - S - \frac{1}{2}(N + P + H)}{C - \frac{1}{2}O - N - S - P} \quad (3)$$

$$NOSC = 4 - \frac{4C + H - 2O - 3N - 2S}{C} \quad (4)$$

C = carbon, H = hydrogen, O = oxygen, N = nitrogen, S = sulfur, P = phosphorus.

2.4 Microbial analyses

2.4.1 DNA extraction and 16S rRNA gene sequencing. To extract pore fluids and corresponding microbial communities, sediment-pore water slurries were centrifuged at 7000 rpm for 10 minutes and the supernatant was then pulled off and filtered through a 0.22 μm filter. DNA was extracted from the filters using the Zymobiomics Quick-DNA Fecal Soil Microbe

Kits (Zymo Research, Ca, USA). For community composition analysis, 16S rRNA genes in the extracted DNA were amplified and sequenced at Argonne National Laboratory (primer set 515F/806R). Raw sequencing data was processed using the QIIME2 pipeline (QIIME2-2019.10), reads were clustered into amplicon sequence variant (ASV) classifications at 99% similarities, and taxonomy was assigned using the QIIME2 scikit-learn classifier trained on the SILVA[79] (release 132) database.[80] All 16S rRNA gene sequencing data is available at NCBI and can be accessed under accession number PRJNA792827. Mean species diversity of each sample (alpha diversity) was calculated based on species abundance and evenness using Shannon's diversity index (*H*), Pielou's evenness (*J*), and species richness (R vegan package).

2.4.2 Metagenomic sequencing and binning. A subset of seven beaver pond sediment samples were selected for metagenomic sequencing to analyze metabolic functional potential within these sediments. Three of these samples were recovered from BP1, 2, and 4, while four other samples were collected from additional beaver wetlands outside the Ryan Fire burn scar (Fig. S1†). Libraries were prepared using the Tecan Ovation Ultralow System V2 and were sequenced on the NovaSEQ6000 platform on a S4 flow cell at Genomics Shared Resource, Colorado Cancer Center, Denver, CO, USA. Sequencing adapters were removed from reads using Bbduk (**https://jgi.doe.gov/data-and-tools/bbtools/bb-tools-user-guide/bbduk-guide/**), and Sickle (v1.33)[81] was used to trim reads. FastQC (v0.11.2) was used before and after trimming reads to ensure high-quality reads were used for downstream processing. Trimmed metagenomic reads are available on NCBI and can be accessed under accession number PRJNA792827. Reads were assembled into contiguous sequences (contigs) using MEGAHIT (v1.2.9)[82] with a minimum kmer of 27, maximum kmer of 127, and step of 10 bp. Assembled contigs greater than 2500 bp were binned using Metabat with default parameters (v2.12.1).[83] We additionally used co-assembly techniques to maximize the number of bins from this dataset. The final metagenome-assembled genomes (MAGs) were assessed for completion and contamination using checkM v1.1.2 (ref. 84) and taxonomy was assigned using GTDB-Tk v1.3.0.[85] The final MAG dataset was combined and dereplicated using dRep v3.0.0 (ref. 86) to create the complete non-redundant database. MAG relative abundance across each sample was calculated using coverM genome v0.6.0 (**https://github.com/wwood/CoverM**). All quality metrics and taxonomy for the 33 medium- and high-quality MAGs discussed here are included in the ESI† (ESI Data 1) and are deposited on Zenodo (**https://doi.org/10.5281/zenodo.5806541**). MAGs were annotated using DRAM v1.2.[87] To identify multiheme c-type cytochromes (MHCs), we used the Geneious Prime (version 2020.0.3) 'Search for motifs' tool to identify protein sequences with at least 3 CXXCH motifs. To remove MHCs not involved with metal reduction, we used the DRAM annotations to remove any sequences annotated as a function likely unassociated with metals. We then analyzed these sequences using PSORTb (v3.0.2)[88] to remove any proteins that were predicted to remain within the cytoplasm.

2.5 Iron analyses

Water samples for ICP-MS were filtered through ashless Whatman paper filters (GE Healthcare) and acidified to 2% HNO_3 prior to analysis. Elemental concentrations of iron (Fe) were measured *via* a NexION 250D mass spectrometer (PerkinElmer, Waltham, MA) connected to a PFA-ST nebulizer (Elemental Scientific, Omaha, Nebraska) and Peltier controlled (PC3x, Elemental Scientific) quartz cyclonic spray chamber (Elemental Scientific) set at 4 °C. Samples were introduced using a prepFAST SC-2 autosampler (Elemental Scientific). The nebulizer gas flow was optimized for maximum Indium signal intensity (58380 counts per second, 0.82 L min^{-1}). To minimize interferences, these measurements were made in dynamic reaction cell mode using ammonia as the reactive gas. Iron concentrations reported represent the sum of the detected concentrations of ^{54}Fe and ^{56}Fe. The detection limits for ^{54}Fe and ^{56}Fe were 7.24 and 6.46 ppb, respectively.

2.6 Statistical analyses

DOC, DTN, %DON, and C : N were evaluated for statistical significance using Student's *t*-test. All burned samples were compared to the unburned sample for these analyses. First, an *F* test was performed to assess the equality of variances between samples. If $F_{calculated}$ (eqn (5) and (6)) is greater than *F* Critical one-tail (determined by degrees of freedom), the difference in variability between measurements is significant, and the variances are unequal; a lower $F_{calculated}$ indicates equal variances.[89] The results of the *F* test were used to inform the appropriate *t*-test (Two-Sample Assuming Equal or Unequal Variances) to determine if the difference in sample means was significant. If *t* Stat (eqn (7) and (8)) is less than *t* critical two-tail (determined by degrees of freedom at 95% confidence interval), the difference is not significant; a higher *t* Stat indicates a significant difference.[89] A significance level of 0.05 was used for statistical significance in all analyses, and all results are reported in Table S2.†

$$F_{\text{calculated}} = \frac{{s_1}^2}{{s_2}^2} \tag{5}$$

$$\text{where } s = \sqrt{\frac{\sum_i \left(x_i - x_{\text{avg}}\right)^2}{n-1}} \tag{6}$$

$$t = \frac{\left|x_{1\text{avg}} - x_{2\text{avg}}\right|}{s_{\text{pooled}}} \sqrt{\frac{n_1 n_2}{n_1 + n_2}} \tag{7}$$

$$\text{where } s_{\text{pooled}} = \sqrt{\frac{{s_1}^2(n_1 - 1) + {s_2}^2(n_2 - 1)}{n_2 + n_2 - 2}} \tag{8}$$

3. Results and discussion

3.1 DOC and DTN increase within beaver ponds

DOC concentrations in the surface grab samples throughout the fire-impacted stream varied on both spatial (Fig. 2a) and temporal scales (Fig. S2†). Average DOC concentrations were

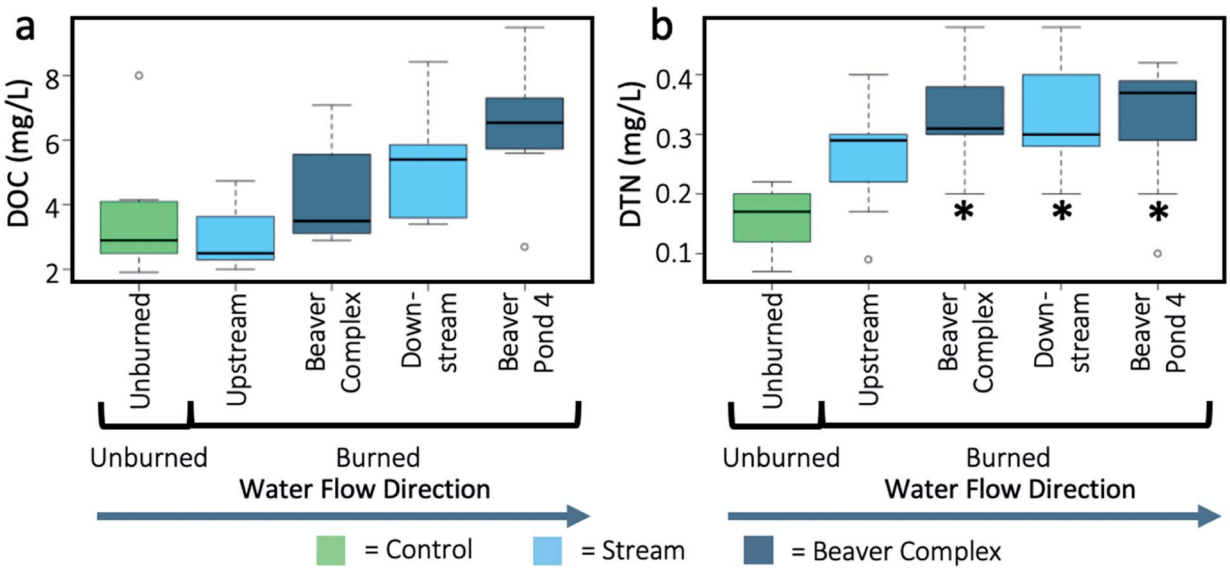

Fig. 2 Dissolved organic carbon (DOC; a) and dissolved total nitrogen (DTN; b) concentrations along a stream impacted by the 2018 Ryan fire and an adjacent unburned stream (Fig. 1). The lower and upper hinges of the boxplots represent the 25th and 75th percentile and the middle line is the median. The upper whisker extends to the median plus 1.5× interquartile range and the lower whisker extends to the median minus 1.5× interquartile range and are comprised of the data from five months of sampling one-year post-fire. Outliers are identified by open circles, and asterisks identify statistical significance.

highest in June 2019 (6.42 ppm, one year after fire, immediately following snow melt) and decreased from June to October (averaging 6.42 ppm to 3.60 ppm, respectively). Such seasonal changes to DOC concentrations have been documented in other high-elevation ecosystems[90] as well as in fire-impacted streams.[15] While DTN averages also varied throughout the summer, the highest average was reported in August 2019 (0.33 ppm) and the lowest in October (0.21 ppm). Seasonal variations in N export agree with changes observed following the 2012 Hayman Fire in Colorado, in which DTN export varied by month.[15]

There was no difference in DOC concentrations between the unburned stream and the burned stream above the beaver ponds (Fig. 2a). DOC roughly doubled and increased steadily as water passed through the sequence of beaver ponds; however, this difference was not significant (Table S2†). Average DTN exhibited a similar trend; the unburned and upstream sites were roughly the same concentrations, and the concentrations in beaver ponds were nearly twice those of the sites preceding them (Table S1†). In contrast with DOC, DTN increases within the ponds were statistically significant (Table S2†). Importantly, the beaver ponds typically contained higher concentrations of DOC and DTN than the site upstream of them (Fig. 2b), in agreement with previous studies conducted on beaver ponds which have shown that these features influence organic C storage by trapping large quantities of sediment and organic material,[91,92] therefore affecting C and N dynamics within those sites.[31] Further evidence of a shift in C and N dynamics is provided by the C : N ratio, which was 32 in the unburned stream and fluctuated between 16–20 in the burned stream (Table S1†). While these differences are not significant (Table S2†), they do represent a shift below the commonly accepted threshold in which microbes are no longer N limited (C : N ratio of 24).[93]

DON constitutes a large percentage of DTN in unburned free-flowing rivers (62–99%).[44] Soil and stream nitrate commonly increase following fire due to decrease of plant uptake, leaching losses and increased nitrification.[94,95] Stream nitrate and DTN were both elevated in watersheds affected by extensive, severe wildfire in ponderosa pine forests in Colorado, but increases in nitrate caused the fraction of DTN comprised by DON to decline from 35% in unburned catchments to 6% in burned catchments.[15] Both nitrate and DTN roughly doubled within the Ryan fire, which indicates minimal wildfire effect on the proportion of DTN comprised by DON. Nitrate decreased by about 40% downstream of the Beaver Complex, consistent with denitrification in the anoxic beaver pond soils (Fig. S3†). The nitrate decline resulted in substantial increases in %DON within the ponds, constituting 60% of DTN in the Beaver Complex and 75% of DTN in BP4 (Table S1†). Although increases in ammonium (NH_4^+) concentrations in rivers following fires have been reported, they were primarily attributed to stormwater events,[42] which were not included in this study. NH_4^+ concentrations reported here showed no appreciable changes on a spatial or temporal scale, remaining very low across the entire sampling gradient, often below 0.01 ppm (Fig. S4†). While only DTN differed significantly (Table S2†) the observed pattern demonstrates N enrichment within the beaver ponds relative to unburned and upstream sites (Table S1†). Local changes in DOC and DTN trends through the stream and beaver ponds may indicate that the influx of pyDOM, among other watershed-derived inputs, into anoxic waters may be less favorable for microbial respiration,[96] leading to localized increases in %DON.

3.2 Nitrogen-containing compounds are enriched within beaver ponds

The elemental class distribution of the surface grab samples for both ionization modes is listed in Fig. 3 (formula counts) and Table 1 (% relative abundances). Within the −ESI spectra, there is an overall decrease in the %CHO and increase in %CHNO between the burned and unburned stream (Table 1), although the CHO fraction still constitutes most formulas assigned (6922 to 9065 formulas and represents 82.2–89.7% of the spectrum). The smallest number of CHO formulas and lowest %CHO were assigned for Beaver Pond 1 (BP1), accompanied by an increase in %CHNO at the site, consistent with the observed increase in DTN in that pond (Fig. 2). The other beaver ponds (BP2, BP3, BP4) also display fewer CHO formulas than the non-beaver pond sites (Unburned, Upstream, Downstream). CHNO variability through the stream resulted in the lowest number of formulas assigned for BP2 (Fig. 3). Importantly, this site also has lower DTN concentrations and a lower %DON than the other beaver ponds (Table S1†). Contrary to other wetland studies, calculated O/C ratios do not appear to be substantially affected by the presence of beaver ponds. Within the sites analyzed here, assigned O/C ratios varied by 0.03 throughout the entire stream (Table S3†), a magnitude of change smaller than that observed in Florida wetlands, where O/C increased by ~0.2.[45] Thus, the observed changes in O/C ratios at the Ryan Fire site are likely not large enough to fundamentally alter the ability of the microbial community to process the pyDOM inputs. To further investigate this, we calculated the nominal oxidative state of carbon (NOSC), which describes a molecule's lability through its direct relationship to the Gibbs free energy (ΔG°) of the reduction half-reaction between organic matter (electron donor) and a terminal electron acceptor (*e.g.*, O_2, NO_3^-, Fe^{3+}, SO_2^{2-}) (eqn (S1)†).[77] NOSC values showed little variation between sampling locations and remained above the thermodynamic limits for standard state (NOSC < −0.6) and sulfidic reduction (NOSC < −0.3)[96] (Table S3†), indicating that thermodynamic limitations associated with oxygen and sulfate reduction (representing the highest and lowest energy yields, respectively) do not apply with respect to NOSC in these samples. Therefore, compositional changes identified through FT-ICR MS are likely not a limiting factor for microbial respiration. However, it is important to note that this value can only be used to predict whether respiration is thermodynamically favorable, and not whether a microbial community is actively transcribing the genes necessary for the breakdown of these compounds.

Complementary +ESI data also displays class element variability throughout the stream (Table 1). The site with the least CHO formulas assigned was Upstream, while the site with the lowest %CHO (66.4%) was Downstream. %CHO steadily declined through each of the successive ponds (BP1, BP2, BP3). This was accompanied by changes in the CHNO fraction, which increased from 3069 formulas Upstream to 8336 in BP 3 (Fig. 3), accompanied by substantial increases in %CHNO. In general, both positive and negative ESI displayed an increase in the number of nitrogenated formulas assigned within the beaver ponds, in conjunction with the increased %DON within those sites (Table S1†). Here, we report more N-containing compounds (Table 1), lower C/N ratios, and higher average N per formula assigned within the beaver ponds compared to the free-flowing sites (Table S4†), evidence for a shift in DOM processing. Previous studies have observed that heterocyclic N-compounds and aromatic N structures are formed and enriched during the heating of soil OM and plant biomass[97–100] that may describe the CHNO species we detected within the beaver ponds.

We compared the tens of thousands of individual elemental compositions identified by FT-ICR MS with van Krevelen diagrams to visualize major shifts in the molecular composition and biological precursor.[56,78,101] For each plot, the mass spectrum was compared to the unburned control, and we subtracted all common formulas between the two spectra. We further refined our analysis to only those formulas that contained N,

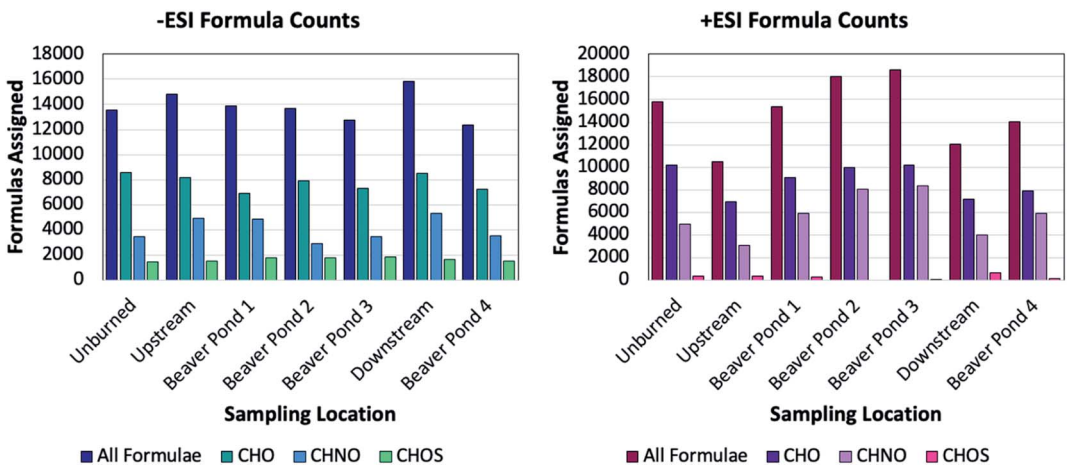

Fig. 3 Elemental composition assignments derived from ± ESI FT-ICR MS at 21 T mass spectra for the Ryan Fire PPL water extracts. Bar charts include the assigned formula counts for each heteroatom class assigned. −ESI bar chart on the left and +ESI bar chart on the right. C = carbon, H = hydrogen, N = nitrogen, O = oxygen, S = sulfur.

Table 1 FT-ICR MS data collected *via* electrospray ionization in negative and positive mode for the Ryan Fire water PPL extracts. % abundance data for −ESI reported on top, +ESI results on the bottom

ESI negative mode	Unburned	Up-stream	Beaver Pond 1	Beaver Pond 2	Beaver Pond 3	Down-stream	Beaver Pond 4
CHO	89.7	84.8	82.2	84.6	84.7	84.2	86
CHNO	6.41	10.3	11.7	10.3	9.5	11.3	9.55
CHOS	3.74	4.69	5.75	4.95	5.68	4.09	4.39
ESI positive mode	Unburned	Up-stream	Beaver Pond 1	Beaver Pond 2	Beaver Pond 3	Down-stream	Beaver Pond 4
CHO	84.6	78.8	75.7	70.6	68.9	66.4	70.9
CHNO	14.8	9.72	17.5	29.4	30.5	14.2	26.9
CHOS	0.385	11.1	6.61	0	0.612	18.7	2.09

using only the +ESI data as this method has been demonstrated to increase the compositional coverage of CHNO species compared to −ESI.[46] We present van Krevelen diagrams that display only these unique nitrogenated species (Fig. 4), which show that CHNO type and quantity differs as the water travels through the stream. Upstream (Fig. 4a), the unique CHNO is centered in the mid-aromatic region. Through the beaver complex, unique CHNO increases in number and expands within the van Krevelen diagram space, first in the aromatic region in BP1 (Fig. 4b), and later covering both the aromatic and aliphatic regions of the van Krevelen diagram (Fig. 4b–d and f). This expansion mirrors the observed increase in DTN and % DON (Table S1†) and indicates that there is regional preservation of CHNO compounds within these ponds, likely due to lower oxygen levels which in turn promote anaerobic metabolism within the microbial community. Indeed, microbial analyses indicate a diversity of putative anaerobic metabolisms within these locations (Fig. 6). Downstream of BP3 the unique

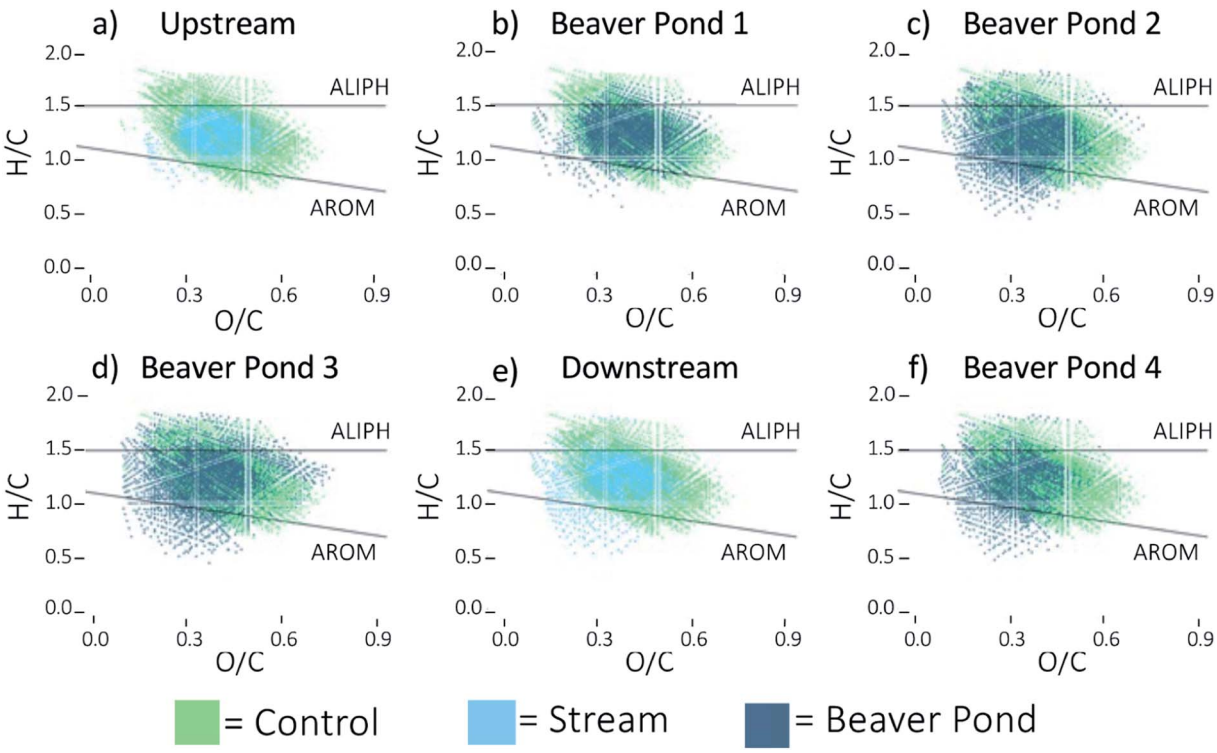

Fig. 4 van Krevelen diagrams plotting the H/C and O/C ratios of the N-containing fraction (*i.e.*, CHNO) obtained *via* +ESI FT-ICR MS of Ryan Fire stream and beaver pond PPL extracts of the unburned control (green) and burned sampling site (blue, see plot title for specific site). Sites are labeled alphabetically through the stream (a–f). Darker blue denotes beaver ponds. Formulas in common are subtracted out, so that only the formulas unique to each sample are plotted. Formulas plotted below the line that intercepts at H/C 1.2 are generally more aromatic in nature, while those plotting above the line that intercepts at 1.5 are more aliphatic.[75]

CHNO rapidly decreases (Fig. 4e) before increasing again in BP4 (Fig. 4f), further indicating that CHNO type and quantity is heavily reliant on its environment and its preservation is indeed highly localized.

3.3 FI and β/α are influenced by fire and wetland presence

FI is commonly used to infer the source of OM (*i.e.*, microbial or terrestrial), where FI = 1.8 indicates microbially-derived DOM and FI = 1.2 indicates terrestrially-derived.[102] While this does not directly measure fire inputs, shifts in FI may represent important differences in microbial processing requirements. We observed an increase in FI values in the surface grab samples through the burned portion of the stream (Fig. S5†) which indicates that fire-influenced DOM more closely resembles microbially-derived DOM, in agreement with previous studies,[53] and is consistent with decreased molecular weight (MW) during the combustion of DOM.[103] This is supported by FT-ICR MS data which indicated that beaver ponds had lower average MW than free-flowing streams (Table S4†). While our FI values for the beaver ponds fall within previously reported ranges for wetlands (approx. 1.3–1.5),[91] there was no appreciable difference between the beaver ponds and the Upstream or Downstream sampling location.

Additionally, β/α is used to infer the proportion of recently produced DOM, in which the beta peak represents recently produced (likely microbial) DOM and the alpha peak represents older, more decomposed DOM.[104] β/α follows a similar trend to FI, increasing with burn activity and remaining elevated throughout the beaver ponds (Fig. S6†). Increases in β/α have been reported following fire[105] and within wetlands,[91] attributed to more simple structures with lower molecular weight and lower dissolved oxygen, respectively.

3.4 Microbial communities drive diverse anaerobic metabolisms in beaver ponds

Fire can have indirect effects on wetland microbes through broad changes in biogeochemistry (*e.g.*, C, N availability). A combination of marker gene (16S rRNA gene) and metagenomic sequencing was used to investigate how the observed changes in aqueous chemistry impacted the microbiomes associated with the beaver pond sediments. 16S rRNA gene sequencing of sediment samples showed that the microbial communities within BP1, 2, and 4 were dominated by the phylum Proteobacteria (average relative abundance of ~35%; Fig. 5a). Within the Proteobacteria, the class Deltaproteobacteria, which is widely known for anaerobic metabolisms[106,107] and frequently identified as one of the most common taxa in wetlands,[108] was the most prevalent throughout the complexes (~20% average relative abundance). Notable orders within the Deltaproteobacteria included Desulforomonadales, Syntrophobacterales, and Desulfobacterales (average relative abundances of 4.4%, 6.5%, and 2%, respectively; Fig. 5b), which include known sulfate reducers and are therefore well-suited for low-oxygen environments, such as beaver ponds.[109]

The microbial communities observed within the Ryan Fire beaver ponds were consistent across additional beaver ponds burned by the Beaver Creek Fire (2016).These nearby wetlands were also dominated by Deltaproteobacteria (~15% average relative abundance) and Desulforomonadales, Syntrophobacterales, and Desulfobacterales orders (4.4%, 3.2% and 1.5% respectively) (Fig. 5), indicating that fresh pyDOM input did not significantly impact the dominant phyla within the beaver ponds. However, the more recently burned (Ryan Fire) beaver pond sediment microbiome was more compositionally diverse than nearby burned soils which were also affected by the same fire and reported elsewhere.[34] Average species richness (number of unique microbial taxa in a sample) within the beaver complexes was approximately double that in nearby burned soils (995 and 503 total species, respectively),[34] likely explained by a combination of factors including significant reductions in soil microbial diversity driven by wildfire events[110,111] and increased DOC and DON complexity within the ponds driven by possible pyDOM inputs.[110,111]

From the metagenomic sequencing of the seven sediment samples, including BP1, 2, and 4, we reconstructed 33 medium and high-quality (>50% complete, <10% contaminated)[112] metagenome-assembled genomes (MAGs), representing the majority of the dominant community members in the corresponding 16S rRNA gene dataset. The MAGs encompassed 12 different phyla, including 14 MAGs from the Desulfobacterota, 7 from the Proteobacteria, and 3 from the Acidobacteria. We linked Deltaproteobacteria amplicon sequence variants (ASVs) with two Desulfobacterota MAGs (with BLAST matches between 16S rRNA gene ASVs and MAG contigs containing 16S rRNA genes of >95% identity over at least 150 bp). We infer that due to known taxonomic inconsistencies between the SILVA and GTDB-TK databases, MAGs classified as Desulfobacterota are taxonomically equivalent to the Deltaproteobacteria ASVs. The Desulfobacterota taxa was dominant in the MAG dataset, accounting for 14 of the 33 MAGs and ~35% of the relative abundance across the three main samples.

Highlighting the distinct chemical conditions found within beaver ponds, we identified a range of putative microbial metabolisms that, in contrast, are generally not observed in fire-impacted soils.[34] We inferred a fermentative lifestyle for several MAGs (*i.e.*, A_BP_metabat.1, All_co_assemble_metabat.86) that encoded a diverse suite of carbohydrate-active enzymes (CAZymes) (Fig. S7†), but which lacked a complete TCA cycle and electron transport chain components (*e.g.*, NADH dehydrogenase, cytochrome C oxidase) (Fig. 6a). Furthermore, these MAGs likely yield fermentation waste products (*e.g.*, short-chain fatty acids) that can be utilized as both C and electron sources by many of the other MAGs (*e.g.*, Desulfobacterota) that perform respiratory metabolisms (Fig. 6d). Indeed, the 14 Desulfobacterota MAGs encoded widespread genomic potential for anaerobic respiratory metabolisms, including metal reduction (*i.e.*, Fe^{3+}, Mn^{4+}), which could drive increased aqueous Fe concentrations in the beaver complexes (Fig. S8†), and potentially cause the observed increases in DOC and DON in the beaver ponds (Fig. 2) and increased number of formulas assigned in the +ESI spectra (Fig. 4) through the dissolution of DOM-metal complexes.[113] This functionality was inferred from the presence of genes encoding multi-heme c-type cytochromes

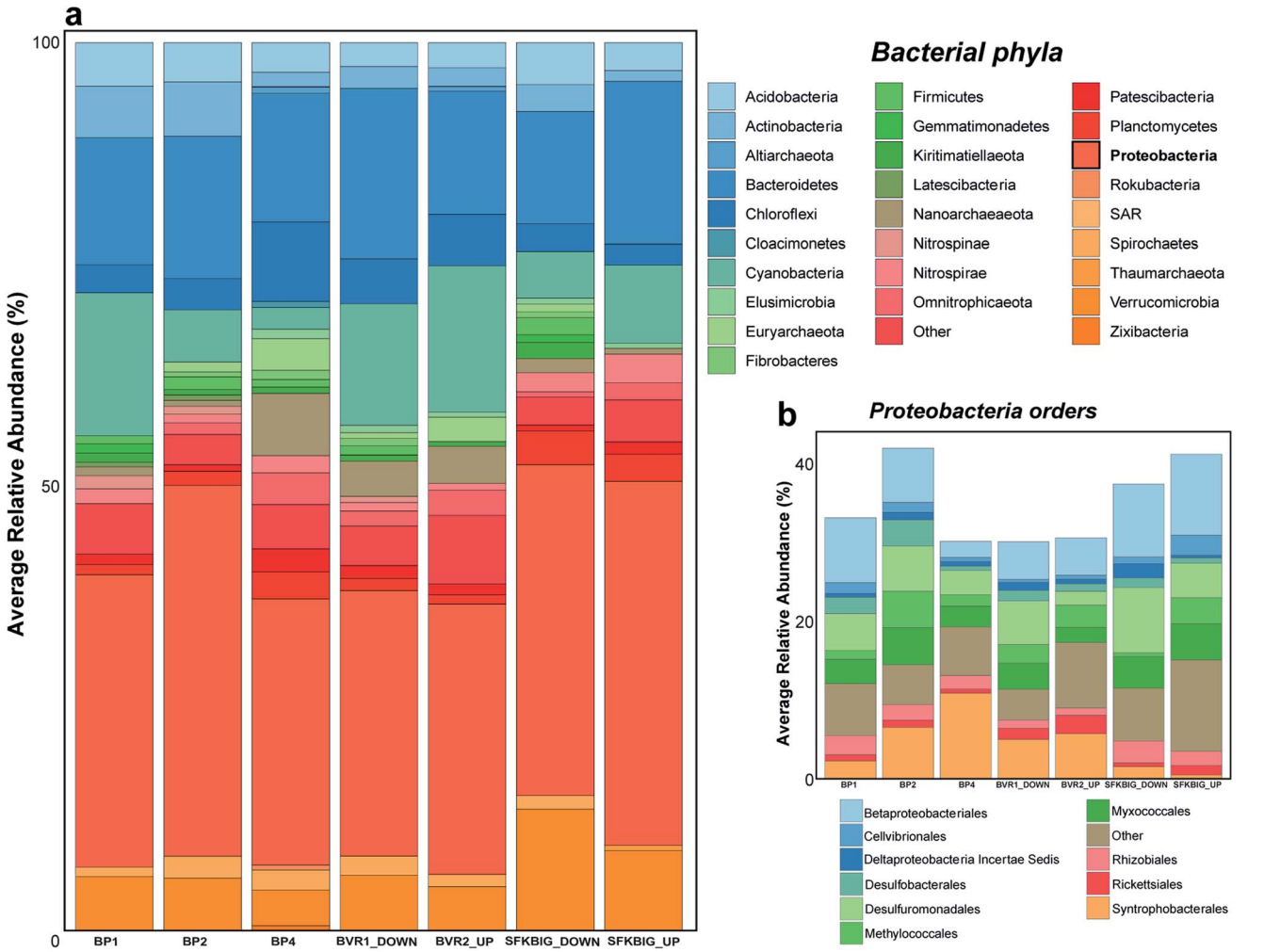

Fig. 5 (a) Bacterial community composition (from 16S rRNA gene sequencing) showing bacterial phyla from beaver pond sediment samples affected by the Ryan fire (2018; BP1, 2, 4) and Beaver Creek fire (2016) (BVR1_DOWN, BVR2_UP, SFKBIG_UP, SFKBIG_DOWN) shown with the relative abundance of dominant bacterial phyla. Community composition is generally consistent across sample sites. (b) The relative abundance of orders within the dominant bacterial phyla, Proteobacteria, across samples. For both a and b, all phyla and orders with average relative abundance <0.005 (0.5%) added to 'Other'.

(MHCs), which are used to transfer electrons to extracellular electron acceptors.[114] Of the 33 recovered MAGs, 29 encoded MHCs, including all 14 of the Desulfobacterota MAGs (Fig. 6c). Eleven of these 14 MAGs had MHCs that could be localized to the periplasm or extracellular space (average of 31 cytochromes per MAG; Fig. 6c), with an average of ~7 CXXCH motifs per cytochrome (range of 3–16), which is similar to iron reducing microorganisms in other systems.[107] Another prevalent anaerobic metabolism is sulfate reduction, identified here through the presence of reductive *dsrAB* genes. Fourteen MAGs – including 10 Desulfobacterota MAGs – encoded these enzymes, further revealing the capacity for diverse metabolisms within the beaver ponds (Fig. 5c). Importantly, our calculated NOSC values indicate that the DOM in the beaver ponds is not energetically constrained from reduction by these alternate electron acceptors (Table S3†)[96] and is a suitable substrate for the wide range of metabolisms identified in the ponds.

Although there is clear evidence for accumulation of unique aromatic compounds within the beaver ponds (Fig. 4), none of the MAGs in this study encoded the enzymatic machinery for anaerobic degradation of aromatic C, which is often formed during soil heating. For example, the enzyme benzylsuccinate synthase (EC:4.1.99.11) that catalyzes fumarate addition as the first step of anaerobic toluene catabolism was absent from all the reconstructed MAGs.[115] Only one MAG (B_BP_metabat.7; phyla Chloroflexota) encoded a benzylsuccinate CoA-transferase subunit (EC:2.8.3.15), which catalyzes the next step of the degradation reaction. Therefore, we infer that the anaerobic degradation of aromatic compounds is likely not a widespread metabolism in the beaver pond microbiome. Because pyDOM is rich in aromatic structures,[116] these results could explain why these molecules appear to be enriched in the low-oxygen beaver ponds (Fig. 4).

Conversely, there is evidence for the potential utilization of other, likely more labile, compounds generated indirectly

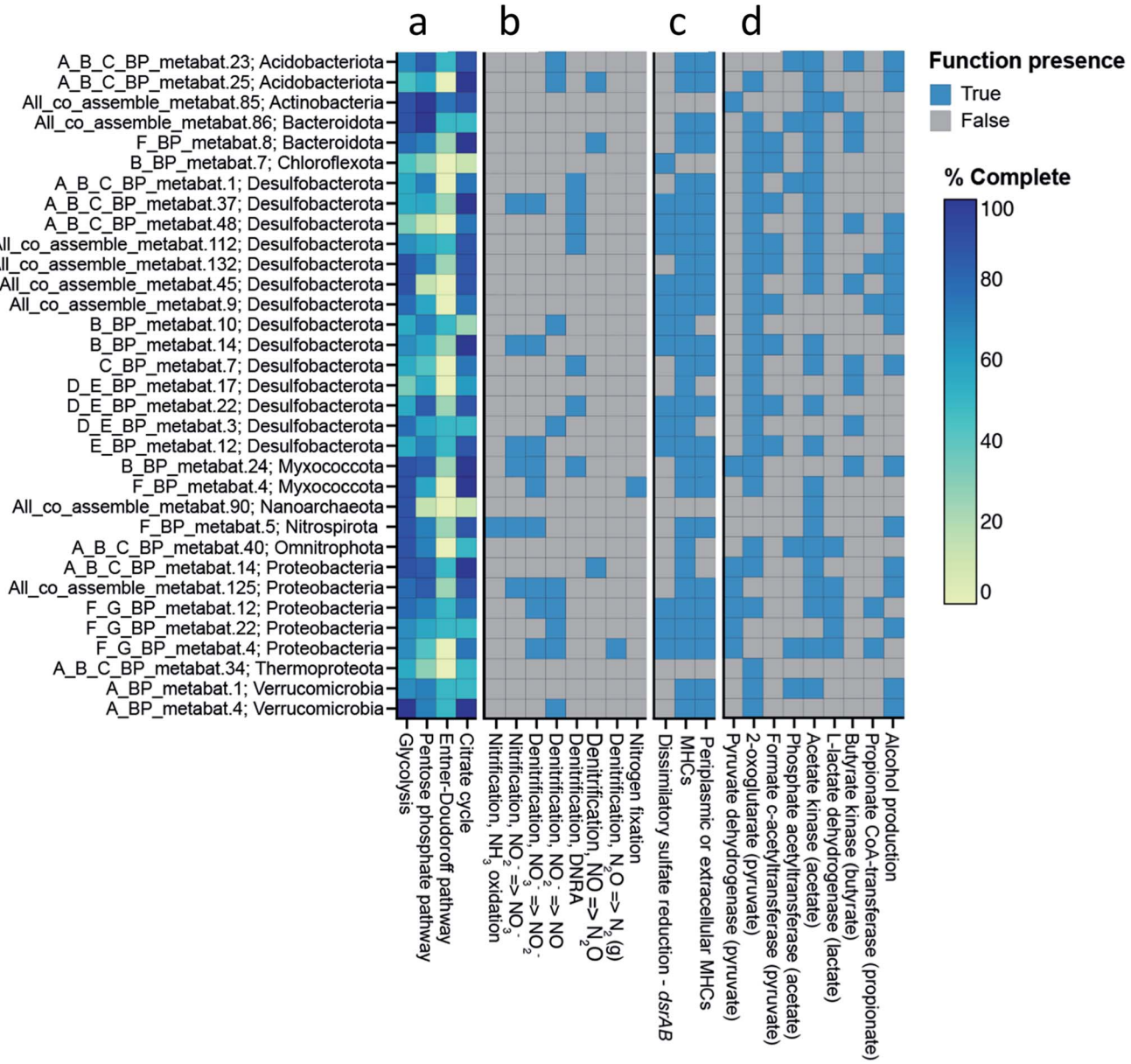

Fig. 6 Broad overview of the (a) completeness or (b–d) presence/absence of functions of interest in the 33 MAGs (listed on the left). Panels overview (a) central metabolism pathways, (b) inorganic N metabolisms, (c) alternate electron acceptors, and (d) SCFA and alcohol conversions. In (d), the compound that the enzyme acts upon is in parentheses. Figure adapted from DRAM product.[87]

following wildfire through microbial degradation of necromass-derived C *via* the utilization of peptidases; all 33 of the MAGs encoded peptidases, with an average of ~116 per genome. Peptidases in the families S33 and C26 were among the most encoded (298 and 219 encoded genes, respectively), similar to other freshwater studies (Wilkins, unpublished data). Peptidases within the S33 family release the N-terminal residue from a peptide, and C26 peptides cleave gamma-linked glutamate bonds. Another top represented family is the M23B family, which contains endopeptidases which lyse bacterial cell wall peptidoglycans. Previous studies have discussed the potential lysing of heat-sensitive cells during fire, which may lead to the release of microbially-derived C after wildfire.[117,118] The encoding of peptidases within our MAG database adds to the hypothesis that post-fire taxa may use this necromass-derived C, which is more labile than aromatic C, following wildfire. From these observations, we infer that the beaver pond microbiome is likely degrading necromass derived from heat-sensitive microbial or invertebrate soil fauna from the surrounding burned watershed,[119] rather than relying on pyDOM or limited vegetation inputs as the primary source of C. Although this has been shown in soils,[34] it has yet to be shown in wetlands within burn scars. These observations also further explain the enrichment of aromatic DOM in the beaver ponds, which is often associated with pyDOM.

The microbial taxa discussed here (*e.g.*, Desulfobacterota) are not typically found in free-flowing freshwater systems[120,121] or fire-impacted soils,[122] demonstrating that microbiomes

within beaver pond sediments have the potential to perform unique biogeochemical reactions within the watershed, thus enhancing the ability of these features to act as ecosystem control points. The functional potential of the dominant community members in these burned beaver complex systems may contribute to Fe mobilization through the stream (Fig. S8†) and highly reducing metabolisms might also facilitate the local sequestration of DOC and DON seen through the complex (Fig. 4). Thus, the implications of potential microbially-mediated heavy metal transformations are a key area for future research in fire-impacted wetlands. While we recognize the relatively small number of samples in our analysis, this study emphasizes the importance of beaver ponds on the biogeochemical processing of burned areas and represents an important step towards understanding how pyDOM is cycled in low-oxygen wetland environments.

4. Conclusions

Water chemistry and microbiology indeed change as water flows through a fire-impacted region, due to the combined influence of fire-impacted organic matter and the presence of beaver ponds along the stream channel. These burned beaver ponds had higher DOC, DTN, and nitrate compared to an upstream reach or an adjacent unburned stream. There was a pattern of increased DOC and DTN within the ponds compared to free-flowing streams, and nitrate appeared to decline as water moved through the sequence of beaver ponds. There were more N-containing formulas detected in the ponds and lower C : N ratios, which would be consistent with increased DTN retention. Additionally, surface water in the beaver ponds had lower C : N ratios and higher aromaticity than burned stream water. Impoundment within beaver ponds may enhance post-fire sediment and C and N storage compared to free-flowing streams, which may minimize the downstream formation of carcinogenic disinfection by-products during chlorination at water treatment plants.[100,123] Microbial analyses indicated that the input of fresh pyDOM did not significantly impact the dominant phyla in the beaver ponds. Rather than using aromatic pyDOM as the primary source of C for respiration, microbes in these sites likely degrade biomass and other more labile sources of organic C. The preservation of pyDOM appeared to be localized within the ponds themselves as changes in elemental composition and unique formulas were limited to the ponds and not observed downstream; therefore, fire-impacted beaver ponds appear to function as biogeochemical "hotspots" due to their unique biogeochemistry.

Conflicts of interest

There are no conflicts to declare.

Acknowledgements

Stream water DOC, DTN was conducted at the Rocky Mountain Research Station, biogeochemistry laboratory, courtesy of the USDA Forest Service. The authors also acknowledge support to MJW and TB from the National Science Foundation under Grant Number 1512670 and USDA National Institute of Food Agriculture through AFRI grant no. 2021-67019034608. This research was funded by the National Science Foundation (2114868) and AFRI grant no. 2021-67019-33726 from the USDA National Institute of Food and Agriculture. A portion of this work was performed at the National High Magnetic Field Laboratory ICR User Facility, which is supported by the National Science Foundation Division of Chemistry and Division of Materials Research through DMR-1644779 and the State of Florida. This work was additionally supported through a grant to MJW, TB and CCR from the Colorado Water Center. TOC art was created with **https://BioRender.com**.

References

1 R. McDonald and D. Shemie, *Urban Water Blueprint: Mapping Conservation Solutions to the Global Water Challenge*, Washington, D.C., 2014.
2 R. de Groot, R. D'Arge, P. Sutton, M. Grasso, K. Limburg, S. Farber, R. Raskin, M. van den Belt, R. Costanza, B. Hannon, J. Paruelo, R. O'Neill and S. Naeem, The Value of the the World's Ecosystem Services and Natural Capital, *Nature*, 2003, **387**, 253–260.
3 S. M. Stein and B. Butler, Private Forests and Public Resources, *Wildland Waters*, 2004, Summer (FS 790), pp. 1–24, DOI: **10.1034/j.1399-3038.2001.012004179-.x**.
4 K. D. Bladon, M. B. Emelko, U. Silins and M. Stone, Wildfire and the Future of Water Supply, *Environ. Sci. Technol.*, 2014, **48**(16), 8936–8943, DOI: **10.1021/es500130g**.
5 M. Ramchander and K. Rahul, Microbial Diversity of Wetlands of India, *Res. J. Chem. Environ.*, 2021, **25**(3), 153–163.
6 M. B. Emelko, U. Silins, K. D. Bladon and M. Stone, Implications of Land Disturbance on Drinking Water Treatability in a Changing Climate: Demonstrating the Need for " Source Water Supply and Protection" Strategies, *Water Res.*, 2011, **45**(2), 461–472, DOI: **10.1016/j.watres.2010.08.051**.
7 M. R. Alizadeh, J. T. Abatzoglou, C. H. Luce, J. F. Adamowski, A. Farid and M. Sadegh, Warming Enabled Upslope Advance in Western US Forest Fires, *Proc. Natl. Acad. Sci. U. S. A.*, 2021, **118**, e2009717118, DOI: **10.1073/pnas.2009717118/-/DCSupplemental**.
8 J. T. Abatzoglou, C. A. Kolden, A. P. Williams, J. A. Lutz and A. M. S. Smith, Climatic Influences on Interannual Variability in Regional Burn Severity across Western US Forests, *Int. J. Wildland Fire*, 2017, **26**(4), 269–275, DOI: **10.1071/WF16165**.
9 H. Knicker, How Does Fire Affect the Nature and Stability of Soil Organic Nitrogen and Carbon? A Review, *Biogeochemistry*, 2007, **85**(1), 91–118, DOI: **10.1007/s10533-007-9104-4**.
10 M. I. Bird, J. G. Wynn, G. Saiz, C. M. Wurster and A. McBeath, The Pyrogenic Carbon Cycle, *Annu. Rev. Earth Planet. Sci.*, 2015, **43**, 273–298, DOI: **10.1146/annurev-earth-060614-105038**.

11 O. Viedma, J. Quesada, I. Torres, A. de Santis and J. M. Moreno, Fire Severity in a Large Fire in a Pinus Pinaster Forest Is Highly Predictable from Burning Conditions, Stand Structure, and Topography, *Ecosystems*, 2015, **18**(2), 237–250, DOI: **10.1007/s10021-014-9824-y**.

12 S. H. Doerr and C. Santín, Global Trends in Wildfire and Its Impacts: Perceptions versus Realities in a Changing World, *Philos. Trans. R. Soc., B*, 2016, **371**, 20150345, DOI: **10.1098/rstb.2015.0345**.

13 M. W. I. Schmidt and A. G. Noack, Black Carbon in Soils and Sediments: Analysis, Distribution, Implications, and Current Challenges, *Global Biogeochem. Cycles*, 2000, **14**(3), 777–793, DOI: **10.1029/1999GB001208**.

14 M. A. Olivella, T. G. Ribalta, A. R. De Febrer, J. M. Mollet and F. X. C. De Las Heras, Distribution of Polycyclic Aromatic Hydrocarbons in Riverine Waters after Mediterranean Forest Fires, *Sci. Total Environ.*, 2006, **355**(1–3), 156–166, DOI: **10.1016/j.scitotenv.2005.02.033**.

15 C. C. Rhoades, A. T. Chow, T. P. Covino, T. S. Fegel, D. N. Pierson and A. E. Rhea, The Legacy of a Severe Wildfire on Stream Nitrogen and Carbon in Headwater Catchments, *Ecosystems*, 2018, **22**, 643–657, DOI: **10.1007/s10021-018-0293-6**.

16 C. C. Rhoades, J. P. Nunes, U. Silins and S. H. Doerr, The Influence of Wildfire on Water Quality and Watershed Processes: New Insights and Remaining Challenges, *Int. J. Wildland Fire*, 2019, **28**(10), 721–725, DOI: **10.1071/WFv28n10_FO**.

17 G. W. Minshall, J. T. Brock, D. A. Andrews and C. T. Robinson, Water Quality, Substratum and Biotic Responses of Five Central Idaho (USA) Streams during the First Year Following the Mortar Creek Fire, *Int. J. Wildland Fire*, 2001, **10**(2), 185–199, DOI: **10.1071/WF01017**.

18 S. F. Murphy, J. H. Writer, R. B. McCleskey and D. A. Martin, The Role of Precipitation Type, Intensity, and Spatial Distribution in Source Water Quality after Wildfire, *Environ. Res. Lett.*, 2015, **10**(8), 079501, DOI: **10.1088/1748-9326/11/7/079501**.

19 A. K. Hohner, K. Cawley, J. Oropeza, R. S. Summers and F. L. Rosario-Ortiz, Drinking Water Treatment Response Following a Colorado Wildfire, *Water Res.*, 2016, **105**, 187–198, DOI: **10.1016/j.watres.2016.08.034**.

20 I. Ferrer, E. M. Thurman, J. A. Zweigenbaum, S. F. Murphy, J. P. Webster and F. L. Rosario-Ortiz, Wildfires: Identification of a New Suite of Aromatic Polycarboxylic Acids in Ash and Surface Water, *Sci. Total Environ.*, 2021, **770**, 144661, DOI: **10.1016/j.scitotenv.2020.144661**.

21 H. G. Smith, G. J. Sheridan, P. N. J. Lane, P. Nyman and S. Haydon, Wildfire Effects on Water Quality in Forest Catchments: A Review with Implications for Water Supply, *J. Hydrol.*, 2011, **396**, 170–192, DOI: **10.1016/j.jhydrol.2010.10.043**.

22 M. Kleber, What Is Recalcitrant Soil Organic Matter?, *Environ. Chem.*, 2010, **7**(4), 320–332, DOI: **10.1071/EN10006**.

23 J. Lehmann and M. Kleber, The Contentious Nature of Soil Organic Matter, *Nature*, 2015, **528**(7580), 60–68, DOI: **10.1038/nature16069**.

24 F. N. Robinne, K. D. Bladon, C. Miller, M. A. Parisien, J. Mathieu and M. D. Flannigan, A Spatial Evaluation of Global Wildfire-Water Risks to Human and Natural Systems, *Sci. Total Environ.*, 2018, **610–611**, 1193–1206, DOI: **10.1016/j.scitotenv.2017.08.112**.

25 R. J. Naiman, C. A. Johnston and J. C. Kelley, Alteration of North American Streams by Beaver, *BioScience*, 1988, **38**(11), 753–762, DOI: **10.2307/1310784**.

26 F. Rosell, O. Bozsér, P. Collen and H. Parker, Ecological Impact of Beavers Castor Fiber and Castor Canadensis and Their Ability to Modify Ecosystems, *Mammal Rev.*, 2005, **35**(3–4), 248–276, DOI: **10.1111/j.1365-2907.2005.00067.x**.

27 M. A. Briggs, C. Wang, F. D. Day-Lewis, K. H. Williams, W. Dong and J. W. Lane, Return Flows from Beaver Ponds Enhance Floodplain-to-River Metals Exchange in Alluvial Mountain Catchments, *Sci. Total Environ.*, 2019, **685**, 357–369, DOI: **10.1016/j.scitotenv.2019.05.371**.

28 K. Boye, A. M. Herrmann, M. v. Schaefer, M. M. Tfaily and S. Fendorf, Discerning Microbially Mediated Processes during Redox Transitions in Flooded Soils Using Carbon and Energy Balances, *Front. Environ. Sci.*, 2018, **6**, 1–14, DOI: **10.3389/fenvs.2018.00015**.

29 A. Larsen, J. R. Larsen and S. N. Lane, Dam Builders and Their Works: Beaver Influences on the Structure and Function of River Corridor Hydrology, Geomorphology, Biogeochemistry and Ecosystems, *Earth-Sci. Rev.*, 2021, **218**, 103623, DOI: **10.1016/j.earscirev.2021.103623**.

30 J. E. C. Missik, H. Liu, Z. Gao, M. Huang, X. Chen, E. Arntzen, D. P. Mcfarland, H. Ren, P. S. Titzler, J. N. Thomle and A. Goldman, Groundwater-River Water Exchange Enhances Growing Season Evapotranspiration and Carbon Uptake in a Semiarid Riparian Ecosystem, *J. Geophys. Res.: Biogeosci.*, 2019, **124**(1), 99–114, DOI: **10.1029/2018JG004666**.

31 L. M. Lynch, T. P. Covino, C. M. Boot, M. D. Wallenstein, N. A. Sutfin and T. S. Fegel, River Channel Connectivity Shifts Metabolite Composition and Dissolved Organic Matter Chemistry, *Nat. Commun.*, 2019, **10**(1), 459, DOI: **10.1038/s41467-019-08406-8**.

32 P. Wegener, T. Covino and C. Rhoades, Evaluating Controls on Nutrient Retention and Export in Wide and Narrow Valley Segments of a Mountain River Corridor, *J. Geophys. Res.: Biogeosci.*, 2018, **123**(6), 1817–1826, DOI: **10.1029/2017JG004109**.

33 M. S. Fischer, F. G. Stark, T. D. Berry, N. Zeba, T. Whitman and M. F. Traxler, Pyrolyzed Substrates Induce Aromatic Compound Metabolism in the Post-Fire Fungus, Pyronema Domesticum, *Front. Microbiol.*, 2021, **12**, 729289, DOI: **10.3389/fmicb.2021.729289**.

34 A. R. Nelson, A. B. Narrowe, C. C. Rhoades, T. S. Fegel, H. K. Roth, R. K. Chu, K. K. Amundson, S. E. Geonczy, R. B. Young, A. S. Steindorff, S. J. Mondo, I. v. Grigoriev, A. Salamov, T. Borch and M. J. Wilkins, Wildfire-dependent changes in soil microbiome diversity and function, *Nat. Microbiol.*, 2022, DOI: **10.1038/s41564-022-01203-y**.

35 C. J. Whitfield, H. M. Baulch, K. P. Chun and C. J. Westbrook, Beaver-Mediated Methane Emission: The Effects of Population Growth in Eurasia and the Americas, *Ambio*, 2015, **44**(1), 7–15, DOI: **10.1007/s13280-014-0575-y**.

36 D. J. Halley, A. P. Saveljev and F. Rosell, Population and Distribution of Beavers Castor Fiber and Castor Canadensis in Eurasia, *Mammal Rev.*, 2021, **51**(1), 1–24, DOI: **10.1111/mam.12216**.

37 D. Geisseler, W. R. Horwath, R. G. Joergensen and B. Ludwig, Pathways of Nitrogen Utilization by Soil Microorganisms - A Review, *Soil Biol. Biochem.*, 2010, **42**, 2058–2067, DOI: **10.1016/j.soilbio.2010.08.021**.

38 C. Acquisti, J. J. Elser and S. Kumar, Ecological Nitrogen Limitation Shapes the DNA Composition of Plant Genomes, *Mol. Biol. Evol.*, 2009, **26**(5), 953–956, DOI: **10.1093/molbev/msp038**.

39 J. Adkins, J. Sanderman and J. Miesel, Soil Carbon Pools and Fluxes Vary across a Burn Severity Gradient Three Years after Wildfire in Sierra Nevada Mixed-Conifer Forest, *Geoderma*, 2019, **333**, 10–22, DOI: **10.1016/j.geoderma.2018.07.009**.

40 J. R. Miesel, W. C. Hockaday, R. K. Kolka and P. A. Townsend, Soil Organic Matter Composition and Quality across Fire Severity Gradients in Coniferous and Deciduous Forests of the Southern Boreal Region, *J. Geophys. Res.: Biogeosci.*, 2015, **120**(6), 1124–1141, DOI: **10.1002/2015JG002959**.

41 C. C. Rhoades, D. Entwistle and D. Butler, The Influence of Wildfire Extent and Severity on Streamwater Chemistry, Sediment and Temperature Following the Hayman Fire, Colorado, *Int. J. Wildland Fire*, 2011, **20**(3), 430–442, DOI: **10.1071/WF09086**.

42 K. D. Bladon, U. Silins, M. J. Wagner, M. Stone, M. B. Emelko, C. A. Mendoza, K. J. Devito and S. Boon, Wildfire Impacts on Nitrogen Concentration and Production from Headwater Streams in Southern Alberta's Rocky Mountains, *Can. J. For. Res.*, 2008, **38**(9), 2359–2371, DOI: **10.1139/X08-071**.

43 F. N. Robinne, K. D. Bladon, U. Silins, M. B. Emelko, M. D. Flannigan, M. A. Parisien, X. Wang, S. W. Kienzle and D. P. Dupont, A Regional-Scale Index for Assessing the Exposure of Drinking-Water Sources to Wildfires, *Forests*, 2019, **10**(5), 1–21, DOI: **10.3390/f10050384**.

44 O. Pisani, J. N. Boyer, D. C. Podgorski, C. R. Thomas, T. Coley and R. Jaffé, Molecular Composition and Bioavailability of Dissolved Organic Nitrogen in a Lake Flow-Influenced River in South Florida, USA, *Aquat. Sci.*, 2017, **79**(4), 891–908, DOI: **10.1007/s00027-017-0540-5**.

45 N. Hertkorn, M. Harir, K. M. Cawley, P. Schmitt-Kopplin and R. Jaffé, Molecular Characterization of Dissolved Organic Matter from Subtropical Wetlands: A Comparative Study through the Analysis of Optical Properties, NMR and FTICR/MS, *Biogeosciences*, 2016, **13**(8), 2257–2277, DOI: **10.5194/bg-13-2257-2016**.

46 H. K. Roth, T. Borch, R. B. Young, W. Bahureksa, G. T. Blakney, A. R. Nelson, M. J. Wilkins and A. M. McKenna, Enhanced Speciation of Pyrogenic Organic Matter from Wildfires Enabled by 21 T FT-ICR Mass Spectrometry, *Anal. Chem.*, 2022, **94**(6), 2973–2980, DOI: **10.1021/acs.analchem.1c05018**.

47 N. T. Jiménez-Morillo, J. M. de la Rosa, D. Waggoner, G. Almendros, F. J. González-Vila and J. A. González-Pérez, Fire Effects in the Molecular Structure of Soil Organic Matter Fractions under Quercus Suber Cover, *Catena*, 2016, **145**, 266–273, DOI: **10.1016/j.catena.2016.06.022**.

48 L. Luo, Z. Chen, J. Lv, Y. Cheng, T. Wu and R. Huang, Molecular Understanding of Dissolved Black Carbon Sorption in Soil-Water Environment, *Water Res.*, 2019, **154**, 210–216, DOI: **10.1016/j.watres.2019.01.060**.

49 J. M. de la Rosa and H. Knicker, Bioavailability of N Released from N-Rich Pyrogenic Organic Matter: An Incubation Study, *Soil Biol. Biochem.*, 2011, **43**(12), 2368–2373, DOI: **10.1016/j.soilbio.2011.08.008**.

50 D. M. Mcknight, E. W. Boyer, P. K. Westerhoff, P. T. Doran, T. Kulbe and D. T. Andersen, Spectrofluorometric Characterization of Dissolved Organic Matter for Indication of Precursor Organic Material and Aromaticity, *Limnol. Oceanogr.*, 2001, **46**, 38–48.

51 R. Jaffé, D. McKnight, N. Maie, R. Cory, W. H. McDowell and J. L. Campbell, Spatial and Temporal Variations in DOM Composition in Ecosystems: The Importance of Long-Term Monitoring of Optical Properties, *J. Geophys. Res.: Biogeosci.*, 2008, **113**(4), 1–15, DOI: **10.1029/2008JG000683**.

52 F. L. Rosario-Ortiz and J. A. Korak, Oversimplification of Dissolved Organic Matter Fluorescence Analysis: Potential Pitfalls of Current Methods, *Environ. Sci. Technol.*, 2017, **51**(2), 759–761, DOI: **10.1021/acs.est.6b06133**.

53 K. M. Cawley, A. K. Hohner, G. A. McKee, T. Borch, P. Omur-Ozbek, J. Oropeza and F. L. Rosario-Ortiz, Characterization and Spatial Distribution of Particulate and Soluble Carbon and Nitrogen from Wildfire-Impacted Sediments, *J. Soils Sediments*, 2018, **18**(4), 1314–1326, DOI: **10.1007/s11368-016-1604-1**.

54 R. M. Cory and D. M. McKnight, Fluorescence Spectroscopy Reveals Ubiquitous Presence of Oxidized and Reduced Quinones in Dissolved Organic Matter, *Environ. Sci. Technol.*, 2005, **39**(21), 8142–8149, DOI: **10.1021/es0506962**.

55 E. Parlanti, K. Woè Rz, L. Geo€roy and M. Lamotte, Dissolved Organic Matter Fluorescence Spectroscopy as a Tool to Estimate Biological Activity in a Coastal Zone Submitted to Anthropogenic Inputs, *Org. Geochem.*, 2000, **31**, 1765–1781, DOI: **10.1016/S0146-6380(00)00124-8**.

56 W. Bahureksa, M. M. Tfaily, R. M. Boiteau, R. B. Young, M. N. Logan, A. M. McKenna and T. Borch, Soil Organic Matter Characterization by Fourier Transform Ion Cyclotron Resonance Mass Spectrometry (FTICR MS): A Critical Review of Sample Preparation, Analysis, and Data Interpretation, *Environ. Sci. Technol.*, 2021, **55**, 9637–9656, DOI: **10.1021/acs.est.1c01135**.

57 N. Hertkorn, M. Frommberger, M. Witt, B. P. Koch, P. Schmitt-Kopplin and E. M. Perdue, Natural Organic Matter and the Event Horizon of Mass Spectrometry, *Anal. Chem.*, 2008, **80**(23), 8908–8919, DOI: **10.1021/ac800464g**.

58 C. L. Hendrickson, J. P. Quinn, N. K. Kaiser, D. F. Smith, G. T. Blakney, T. Chen, A. G. Marshall, C. R. Weisbrod and S. C. Beu, 21 Tesla Fourier Transform Ion Cyclotron Resonance Mass Spectrometer: A National Resource for Ultrahigh Resolution Mass Analysis, *J. Am. Soc. Mass Spectrom.*, 2015, **26**(9), 1626–1632, DOI: **10.1007/s13361-015-1182-2**.

59 T. Ohno, R. L. Sleighter and P. G. Hatcher, Comparative Study of Organic Matter Chemical Characterization Using Negative and Positive Mode Electrospray Ionization Ultrahigh-Resolution Mass Spectrometry, *Anal. Bioanal. Chem.*, 2016, **408**(10), 2497–2504, DOI: **10.1007/s00216-016-9346-x**.

60 T. Dittmar, B. Koch, N. Hertkorn and G. Kattner, A Simple and Efficient Method for the Solid-Phase Extraction of Dissolved Organic Matter (SPE-DOM) from Seawater, *Limnol. Oceanogr.: Methods*, 2008, **6**, 230–235.

61 B. Lam, A. Baer, M. Alaee, B. Lefebvre, A. Moser, A. Williams and A. J. Simpson, Major Structural Components in Freshwater Dissolved Organic Matter, *Environ. Sci. Technol.*, 2007, **41**(24), 8240–8247, DOI: **10.1021/es0713072**.

62 Y. Li, M. Harir, J. Uhl, B. Kanawati, M. Lucio, K. S. Smirnov, B. P. Koch, P. Schmitt-Kopplin and N. Hertkorn, How Representative Are Dissolved Organic Matter (DOM) Extracts? A Comprehensive Study of Sorbent Selectivity for DOM Isolation, *Water Res.*, 2017, **116**, 316–323, DOI: **10.1016/j.watres.2017.03.038**.

63 M. R. Emmett, F. M. White, C. L. Hendrickson, D. H. Shi and A. G. Marshall, Application of Micro-Electrospray Liquid Chromatography Techniques to FT-ICR MS to Enable High-Sensitivity Biological Analysis, *J. Am. Soc. Mass Spectrom.*, 1998, **9**(4), 333–340, DOI: **10.1016/S1044-0305(97)00287-0**.

64 D. F. Smith, D. C. Podgorski, R. P. Rodgers, G. T. Blakney and C. L. Hendrickson, 21 Tesla FT-ICR Mass Spectrometer for Ultrahigh-Resolution Analysis of Complex Organic Mixtures, *Anal. Chem.*, 2018, **90**(3), 2041–2047, DOI: **10.1021/acs.analchem.7b04159**.

65 N. K. Kaiser, A. M. McKenna, J. J. Savory, C. L. Hendrickson and A. G. Marshall, Tailored Ion Radius Distribution for Increased Dynamic Range in FT-ICR Mass Analysis of Complex Mixtures, *Anal. Chem.*, 2013, **85**(1), 265–272, DOI: **10.1021/ac302678v**.

66 T. Chen, S. C. Beu, N. K. Kaiser and C. L. Hendrickson, Note: Optimized Circuit for Excitation and Detection with One Pair of Electrodes for Improved Fourier Transform Ion Cyclotron Resonance Mass Spectrometry, *Rev. Sci. Instrum.*, 2014, **85**(6), 066107, DOI: **10.1063/1.4883179**.

67 I. A. Boldin and E. N. Nikolaev, Fourier Transform Ion Cyclotron Resonance Cell with Dynamic Harmonization of the Electric Field in the Whole Volume by Shaping of the Excitation and Detection Electrode Assembly, *Rapid Commun. Mass Spectrom.*, 2011, **25**(1), 122–126, DOI: **10.1002/rcm.4838**.

68 G. T. Blakney, C. L. Hendrickson and A. G. Marshall, Predator Data Station: A Fast Data Acquisition System for Advanced FT-ICR MS Experiments, *Int. J. Mass Spectrom.*, 2011, **306**(2–3), 246–252, DOI: **10.1016/j.ijms.2011.03.009**.

69 F. Xian, C. L. Hendrickson, G. T. Blakney, S. C. Beu and A. G. Marshall, Automated Broadband Phase Correction of Fourier Transform Ion Cyclotron Resonance Mass Spectra, *Anal. Chem.*, 2010, **82**(21), 8807–8812, DOI: **10.1021/ac101091w**.

70 J. J. Savory, N. K. Kaiser, A. M. Mckenna, F. Xian, G. T. Blakney, R. P. Rodgers, C. L. Hendrickson and A. G. Marshall, Measurement Accuracy with a "Walking" Calibration Equation, *Anal. Chem.*, 2011, **83**, 1732–1736.

71 E. Kendrick, A Mass Scale Based Resolution Mass Spectrometry of Organic Compounds, *Anal. Chem.*, 1963, **35**(13), 2146–2154.

72 C. A. Hughey, C. L. Hendrickson, R. P. Rodgers, A. G. Marshall and K. Qian, Kendrick Mass Defect Spectrum: A Compact Visual Analysis for Ultrahigh-Resolution Broadband Mass Spectra, *Anal. Chem.*, 2001, **73**(19), 4676–4681, DOI: **10.1021/ac010560w**.

73 F. W. McLafferty and F. Turecek, *Interpretation of Mass Spectra*, University Science Books, Mill Valley, CA, 4th edn, 1993.

74 Y. E. Corilo, *PetroOrg Software*, Florida State University, Omics LLC, Tallahassee, FL, 2014.

75 B. P. Koch and T. Dittmar, From Mass to Structure: An Aromaticity Index for High-Resolution Mass Data of Natural Organic Matter, *Rapid Commun. Mass Spectrom.*, 2006, **20**(5), 926–932, DOI: **10.1002/rcm.2386**.

76 B. P. Koch and T. Dittmar, Erratum: From Mass to Structure: An Aromaticity Index for High-Resolution Mass Data of Natural Organic Matter, *Rapid Commun. Mass Spectrom.*, 2006, **20**, 926–932, DOI: **10.1002/Rcm.2386**.

77 D. E. LaRowe and P. Van Cappellen, Degradation of Natural Organic Matter: A Thermodynamic Analysis, *Geochim. Cosmochim. Acta*, 2011, **75**(8), 2030–2042, DOI: **10.1016/j.gca.2011.01.020**.

78 S. Kim, R. W. Kramer and P. G. Hatcher, Graphical Method for Analysis of Ultrahigh-Resolution Broadband Mass Spectra of Natural Organic Matter, the Van Krevelen Diagram, *Anal. Chem.*, 2003, **75**(20), 5336–5344, DOI: **10.1021/ac034415p**.

79 C. Quast, E. Pruesse, P. Yilmaz, J. Gerken, T. Schweer, P. Yarza, J. Peplies and F. O. Glöckner, The SILVA Ribosomal RNA Gene Database Project: Improved Data Processing and Web-Based Tools, *Nucleic Acids Res.*, 2012, **41**(D1), D590–D596, DOI: **10.1093/nar/gks1219**.

80 C. Quast, E. Pruesse, P. Yilmaz, J. Gerken, T. Schweer, P. Yarza, J. Peplies and F. O. Glöckner, The SILVA Ribosomal RNA Gene Database Project: Improved Data Processing and Web-Based Tools, *Nucleic Acids Res.*, 2013, **41**, D590–D596, DOI: **10.1093/nar/gks1219**.

81 N. Joshi and J. Fass, *Sickle: A Sliding-Window, Adaptive, Quality-Based Trimming Tool for FastQ Files*, 2011.

82 D. Li, C. M. Liu, R. Luo, K. Sadakane and T. W. Lam, MEGAHIT: An Ultra-Fast Single-Node Solution for Large and Complex Metagenomics Assembly via Succinct de

Bruijn Graph, *Bioinformatics*, 2015, **31**(10), 1674–1676, DOI: **10.1093/bioinformatics/btv033**.

83 D. D. Kang, F. Li, E. Kirton, A. Thomas, R. Egan, H. An and Z. Wang, MetaBAT 2: An Adaptive Binning Algorithm for Robust and Efficient Genome Reconstruction from Metagenome Assemblies, *PeerJ*, 2019, (7), DOI: **10.7717/peerj.7359**.

84 D. H. Parks, M. Imelfort, C. T. Skennerton, P. Hugenholtz and G. W. Tyson, CheckM.: Assessing the Quality of Microbial Genomes Recovered from Isolates, Single Cells, and Metagenomes, *Genome Res.*, 2015, **25**(7), 1043–1055, DOI: **10.1101/gr.186072.114**.

85 P. A. Chaumeil, A. J. Mussig, P. Hugenholtz and D. H. Parks, GTDB-Tk: A Toolkit to Classify Genomes with the Genome Taxonomy Database, *Bioinformatics*, 2020, **36**(6), 1925–1927, DOI: **10.1093/bioinformatics/btz848**.

86 M. R. Olm, C. T. Brown, B. Brooks and J. F. Banfield, DRep: A Tool for Fast and Accurate Genomic Comparisons That Enables Improved Genome Recovery from Metagenomes through de-Replication, *ISME J.*, 2017, **11**(12), 2864–2868, DOI: **10.1038/ismej.2017.126**.

87 M. Shaffer, M. A. Borton, B. B. McGivern, A. A. Zayed, S. L. la Rosa, L. M. Solden, P. Liu, A. B. Narrowe, J. Rodríguez-Ramos, B. Bolduc, M. C. Gazitúa, R. A. Daly, G. J. Smith, D. R. Vik, P. B. Pope, M. B. Sullivan, S. Roux and K. C. Wrighton, DRAM for Distilling Microbial Metabolism to Automate the Curation of Microbiome Function, *Nucleic Acids Res.*, 2020, **48**(16), 8883–8900, DOI: **10.1093/nar/gkaa621**.

88 N. Y. Yu, J. R. Wagner, M. R. Laird, G. Melli, S. Rey, R. Lo, P. Dao, S. Cenk Sahinalp, M. Ester, L. J. Foster and F. S. L. Brinkman, PSORTb 3.0: Improved Protein Subcellular Localization Prediction with Refined Localization Subcategories and Predictive Capabilities for All Prokaryotes, *Bioinformatics*, 2010, **26**(13), 1608–1615, DOI: **10.1093/bioinformatics/btq249**.

89 D. C. Harris, *Exploring Chemical Analysis*, ed. Fiorillo, J., Murphy, B., Hadler, G. L., Simpson, J. and Szczepanski, T., W.H. Freeman and Company, New York, fifth edn, 2013.

90 S. Wagner, R. Jaffé, K. Cawley, T. Dittmar and A. Stubbins, Associations between the Molecular and Optical Properties of Dissolved Organic Matter in the Florida Everglades, a Model Coastal Wetland System, *Front. Chem.*, 2015, **3**, 1–14, DOI: **10.3389/fchem.2015.00066**.

91 N. Catalán, S. Herrero Ortega, H. Gröntoft, T. G. Hilmarsson, S. Bertilsson, P. Wu, O. Levanoni, K. Bishop and A. G. Bravo, Effects of Beaver Impoundments on Dissolved Organic Matter Quality and Biodegradability in Boreal Riverine Systems, *Hydrobiologia*, 2017, **793**(1), 135–148, DOI: **10.1007/s10750-016-2766-y**.

92 P. Nummi, M. Vehkaoja, J. Pumpanen and A. Ojala, Beavers Affect Carbon Biogeochemistry: Both Short-Term and Long-Term Processes Are Involved, *Mammal Rev.*, 2018, **48**(4), 298–311, DOI: **10.1111/mam.12134**.

93 G. E. Brust, Management Strategies for Organic Vegetable Fertility, in *Safety and Practice for Organic Food*, Elsevier, 2019, pp. 193–212, DOI: **10.1016/B978-0-12-812060-6.00009-X**.

94 G. Certini, Effects of Fire on Properties of Forest Soils: A Review, *Oecologia*, 2005, **143**(1), 1–10, DOI: **10.1007/s00442-004-1788-8**.

95 S. Wan, D. Hui and Y. Luo, Fire effects on nitrogen pools and dynamics in terrestrial ecosystems: a meta-analysis, *Ecol. Appl.*, 2001, **11**(5), 1349–1365.

96 V. Noël, M. M. Tfaily, S. Fendorf, S. E. Bone, K. Boye, K. H. Williams and J. R. Bargar, Thermodynamically Controlled Preservation of Organic Carbon in Floodplains, *Nat. Geosci.*, 2017, **10**(6), 415–419, DOI: **10.1038/ngeo2940**.

97 J. M. de La Rosa, A. Z. Miller and H. Knicker, Soil-Borne Fungi Challenge the Concept of Long-Term Biochemical Recalcitrance of Pyrochar, *Sci. Rep.*, 2018, **8**(1), 1–9, DOI: **10.1038/s41598-018-21257-5**.

98 S. R. Faria, J. M. de la Rosa, H. Knicker, J. A. González-Pérez and J. J. Keizer, Molecular Characterization of Wildfire Impacts on Organic Matter in Eroded Sediments and Topsoil in Mediterranean Eucalypt Stands, *Catena*, 2015, **135**, 29–37, DOI: **10.1016/j.catena.2015.07.007**.

99 H. Knicker, F. J. González-Vila, O. Polvillo, J. A. González and G. Almendros, Fire-Induced Transformation of C- and N- Forms in Different Organic Soil Fractions from a Dystric Cambisol under a Mediterranean Pine Forest (Pinus Pinaster), *Soil Biol. Biochem.*, 2005, **37**(4), 701–718, DOI: **10.1016/j.soilbio.2004.09.008**.

100 W. Bahureksa, R. B. Young, A. M. McKenna, H. Chen, K. A. Thorn, F. L. Rosario-Ortiz and T. Borch, Nitrogen Enrichment during Soil Organic Matter Burning and Molecular Evidence of Maillard Reactions, *Environ. Sci. Technol.*, 2022, **56**(7), 4597–4609, DOI: **10.1021/acs.est.1c06745**.

101 A. Rivas-Ubach, Y. Liu, T. S. Bianchi, N. Tolić, C. Jansson and L. Paša-Tolić, Moving beyond the van Krevelen Diagram: A New Stoichiometric Approach for Compound Classification in Organisms, *Anal. Chem.*, 2018, **90**(10), 6152–6160, DOI: **10.1021/acs.analchem.8b00529**.

102 L. Wang, Y. Chen, S. Chen, L. Long, Y. Bu, H. Xu, B. Chen and S. Krasner, A One-Year Long Survey of Temporal Disinfection Byproducts Variations in a Consumer's Tap and Their Removals by a Point-of-Use Facility, *Water Res.*, 2019, **159**, 203–213, DOI: **10.1016/j.watres.2019.04.062**.

103 C. Romera-Castillo, M. Chen, Y. Yamashita and R. Jaffé, Fluorescence Characteristics of Size-Fractionated Dissolved Organic Matter: Implications for a Molecular Assembly Based Structure?, *Water Res.*, 2014, **55**, 40–51, DOI: **10.1016/j.watres.2014.02.017**.

104 A. M. Hansen, T. E. C. Kraus, B. A. Pellerin, J. A. Fleck, B. D. Downing and B. A. Bergamaschi, Optical Properties of Dissolved Organic Matter (DOM): Effects of Biological and Photolytic Degradation, *Limnol. Oceanogr.*, 2016, **61**(3), 1015–1032, DOI: **10.1002/lno.10270**.

105 J. J. Wang, R. A. Dahlgren, M. S. Erşan, T. Karanfil and A. T. Chow, Wildfire Altering Terrestrial Precursors of Disinfection Byproducts in Forest Detritus, *Environ. Sci.*

Technol., 2015, **49**(10), 5921–5929, DOI: **10.1021/es505836m**.

106 L. M. Jochum, L. Schreiber, I. P. G. Marshall, B. B. Jørgensen, A. Schramm and K. U. Kjeldsen, Single-Cell Genomics Reveals a Diverse Metabolic Potential of Uncultivated Desulfatiglans-Related Deltaproteobacteria Widely Distributed in Marine Sediment, *Front. Microbiol.*, 2018, **9**, 2038, DOI: **10.3389/fmicb.2018.02038**.

107 R. E. Danczak, M. D. Johnston, C. Kenah, M. Slattery and M. J. Wilkins, Capability for Arsenic Mobilization in Groundwater Is Distributed across Broad Phylogenetic Lineages, *PLoS One*, 2019, **14**(9), e0221694, DOI: **10.1371/journal.pone.0221694**.

108 B. S. Abraham, D. Caglayan, N. v. Carrillo, M. C. Chapman, C. T. Hagan, S. T. Hansen, R. O. Jeanty, A. A. Klimczak, M. J. Klingler, T. P. Kutcher, S. H. Levy, A. A. Millard-Bruzos, T. B. Moore, D. J. Prentice, M. E. Prescott, R. Roehm, J. A. Rose, M. Yin, A. Hyodo, K. Lail, C. Daum, A. Clum, A. Copeland, R. Seshadri, T. G. del Rio, E. A. Eloe-Fadrosh and J. B. Benskin, Shotgun Metagenomic Analysis of Microbial Communities from the Loxahatchee Nature Preserve in the Florida Everglades, *Environ. Microbiome.*, 2020, **15**(1), 2, DOI: **10.1186/s40793-019-0352-4**.

109 M. Pester, K. H. Knorr, M. W. Friedrich, M. Wagner and A. Loy, Sulfate-Reducing Microorganisms in Wetlands - Fameless Actors in Carbon Cycling and Climate Change, *Front. Microbiol.*, 2012, **3**, 72, DOI: **10.3389/fmicb.2012.00072**.

110 L. E. Sáenz de Miera, R. Pinto, J. J. Gutierrez-Gonzalez, L. Calvo and G. Ansola, Wildfire Effects on Diversity and Composition in Soil Bacterial Communities, *Sci. Total Environ.*, 2020, **726**, 138636, DOI: **10.1016/j.scitotenv.2020.138636**.

111 T. Whitman, E. Whitman, J. Woolet, M. D. Flannigan, D. K. Thompson and M. A. Parisien, Soil Bacterial and Fungal Response to Wildfires in the Canadian Boreal Forest across a Burn Severity Gradient, *Soil Biol. Biochem.*, 2019, **138**, 107571, DOI: **10.1016/j.soilbio.2019.107571**.

112 R. M. Bowers, N. C. Kyrpides, R. Stepanauskas, M. Harmon-Smith, D. Doud, T. B. K. Reddy, F. Schulz, J. Jarett, A. R. Rivers, E. A. Eloe-Fadrosh, S. G. Tringe, N. N. Ivanova, A. Copeland, A. Clum, E. D. Becraft, R. R. Malmstrom, B. Birren, M. Podar, P. Bork, G. M. Weinstock, G. M. Garrity, J. A. Dodsworth, S. Yooseph, G. Sutton, F. O. Glöckner, J. A. Gilbert, W. C. Nelson, S. J. Hallam, S. P. Jungbluth, T. J. G. Ettema, S. Tighe, K. T. Konstantinidis, W. T. Liu, B. J. Baker, T. Rattei, J. A. Eisen, B. Hedlund, K. D. McMahon, N. Fierer, R. Knight, R. Finn, G. Cochrane, I. Karsch-Mizrachi, G. W. Tyson, C. Rinke, A. Lapidus, F. Meyer, P. Yilmaz, D. H. Parks, A. M. Eren, L. Schriml, J. F. Banfield, P. Hugenholtz and T. Woyke, Minimum Information about a Single Amplified Genome (MISAG) and a Metagenome-Assembled Genome (MIMAG) of Bacteria and Archaea, *Nat. Biotechnol.*, 2017, **25**(8), 725–731, DOI: **10.1038/nbt.3893**.

113 M. S. Patzner, C. W. Mueller, M. Malusova, M. Baur, V. Nikeleit, T. Scholten, C. Hoeschen, J. M. Byrne, T. Borch, A. Kappler and C. Bryce, Iron Mineral Dissolution Releases Iron and Associated Organic Carbon during Permafrost Thaw, *Nat. Commun.*, 2020, **11**(1), 6329, DOI: **10.1038/s41467-020-20102-6**.

114 S. Sharma, G. Cavallaro and A. Rosato, A Systematic Investigation of Multiheme C-Type Cytochromes in Prokaryotes, *J. Biol. Inorg. Chem.*, 2010, **15**(4), 559–571, DOI: **10.1007/s00775-010-0623-4**.

115 G. Fuchs, M. Boll and J. Heider, Microbial Degradation of Aromatic Compounds- From One Strategy to Four, *Nat. Rev. Microbiol.*, 2011, **9**(11), 803–816, DOI: **10.1038/nrmicro2652**.

116 H. Knicker, A. Hilscher, J. M. de la Rosa, J. A. González-Pérez and F. J. González-Vila, Modification of Biomarkers in Pyrogenic Organic Matter during the Initial Phase of Charcoal Biodegradation in Soils, *Geoderma*, 2013, **197–198**, 43–50, DOI: **10.1016/j.geoderma.2012.12.021**.

117 J. Donhauser, P. A. Niklaus, J. Rousk, C. Larose and B. Frey, Temperatures beyond the Community Optimum Promote the Dominance of Heat-Adapted, Fast Growing and Stress Resistant Bacteria in Alpine Soils, *Soil Biol. Biochem.*, 2020, **148**, 107873, DOI: **10.1016/j.soilbio.2020.107873**.

118 J. Donhauser, W. Qi, B. Bergk-Pinto and B. Frey, High Temperatures Enhance the Microbial Genetic Potential to Recycle C and N from Necromass in High-Mountain Soils, *Global Change Biol.*, 2021, **27**(7), 1365–1386, DOI: **10.1111/gcb.15492**.

119 T. D. Bruns, J. A. Chung, A. A. Carver and S. I. Glassman, A Simple Pyrocosm for Studying Soil Microbial Response to Fire Reveals a Rapid, Massive Response by Pyronema Species, *PLoS One*, 2020, **15**(3), 1–20, DOI: **10.1371/journal.pone.0222691**.

120 A. R. Nelson, A. H. Sawyer, R. S. Gabor, C. M. Saup, S. R. Bryant, K. D. Harris, M. A. Briggs, K. H. Williams and M. J. Wilkins, Heterogeneity in Hyporheic Flow, Pore Water Chemistry, and Microbial Community Composition in an Alpine Streambed, *J. Geophys. Res.: Biogeosci.*, 2019, **124**(11), 3465–3478, DOI: **10.1029/2019JG005226**.

121 C. M. Saup, S. R. Bryant, A. R. Nelson, K. D. Harris, A. H. Sawyer, J. N. Christensen, M. M. Tfaily, K. H. Williams and M. J. Wilkins, Hyporheic Zone Microbiome Assembly Is Linked to Dynamic Water Mixing Patterns in Snowmelt-Dominated Headwater Catchments, *J. Geophys. Res.: Biogeosci.*, 2019, **124**(11), 3269–3280, DOI: **10.1029/2019JG005189**.

122 C. F. Weber, J. S. Lockhart, E. Charaska, K. Aho and K. A. Lohse, Bacterial Composition of Soils in Ponderosa Pine and Mixed Conifer Forests Exposed to Different Wildfire Burn Severity, *Soil Biol. Biochem.*, 2014, **69**, 242–250, DOI: **10.1016/j.soilbio.2013.11.010**.

123 J. J. Wang, R. A. Dahlgren, M. S. Erşan, T. Karanfil and A. T. Chow, Temporal Variations of Disinfection Byproduct Precursors in Wildfire Detritus, *Water Res.*, 2016, **99**, 66–73, DOI: **10.1016/j.watres.2016.04.030**.